universität wien

MASTERARBEIT / MASTER'S THESIS

Titel der Masterarbeit / Title of the Master's Thesis

„Quantification of sanggenons from white mulberry root bark extracts and murine biomatrices after oral administration"

verfasst von / submitted by

Sabrina Lag, BSc

angestrebter akademischer Grad / in partial fulfilment of the requirements for the degree of

Magistra pharmaciae (Mag.pharm.)

Wien, 2022 / Vienna 2022

Studienkennzahl lt. Studienblatt / degree programme code as it appears on the student record sheet:	UA 066 605
Studienrichtung lt. Studienblatt / degree programme as it appears on the student record sheet:	Masterstudium Pharmazie
Betreut von / Supervisor:	Univ.-Prof. Mag. Dr. Judith Maria Rollinger

ACKNOWLEDGEMENTS

My special gratefulness is dedicated to Univ.-Prof. Mag. Dr. Judith Maria Rollinger for giving me the opportunity to perform my Master thesis in her working group 'Phytochemistry and Biodiscovery' in the Division of Pharmacognosy, University of Vienna, and to get an insight into pharmacognostic research. I would like to thank her and my co-supervisor Priv.-Doz. Mag. Dr. Ulrike Grienke for their great support and valuable advices during the progress of my work. Also, many thanks to Dr. Ammar Tahir, MSc, for his beneficial assistance with this project.

Further, my great gratitude goes to the best co-supervisor one could only wish for: Mag. pharm. Julia Langeder. With her experience she perfectly guided me through the experiments. Her helpfulness, patience and cheerfulness are quite fascinating and made working with her truly pleasant and enjoyable. Thanks for your great support and I am glad to getting to know you, Julia.

I am especially thankful to the whole research group of Prof. Rollinger for their kind reception in their team and their cooperativeness – I immediately felt comfortable. Also, there were always very amusing and pleasant lunch breaks that I would not want to have missed.

Most of all, I am extremely grateful for the great support from my parents Ulrike and Eduard and my sister Verena, who have made a huge contribution to achieving my goal and have always had faith in me. Special gratitude I owe my boyfriend Thomas for always being by my side on this long journey. He took the role of a motivational coach who always believed in me. I extremely appreciate your patience and support. Last but not least, thanks to my study colleagues which became real friends over the years. Numerous hours of learning together and funny, enjoyably and culinarily evenings welded us together closely – I am very thankful to know you! ☺

TABLE OF CONTENT

ABSTRACT

The influenza virus is responsible for numerous severe respiratory illnesses and deaths worldwide every year. In case of a secondary infection, e.g. with *Streptococcus pneumoniae,* the synergism of the virus and bacteria leads to severe health complications. Therefore, a dual mechanism of both antiviral and antibacterial properties could decrease morbidity and mortality rates. Prenylated flavonoids, particularly the complex Diels-Alder-type adducts contained in the root bark of *Morus alba* L., have been shown previously to act as dual inhibitors in *in vitro* studies and are promising candidates to disrupt the lethal synergism of influenza virus and *S. pneumoniae in vivo*.

This master thesis deals with two research projects. The first focuses on the quantification of Diels-Alder-type adducts, in particular kuwanon L_{130A} [**1**], sanggenon D [**2**], sanggenon B [**3**], sanggenon G [**4**], sanggenon O [**5**], sanggenon E [**6**], sanggenon C [**7**] by using ultra-performance liquid chromatography (UPLC) in specialized accelerated solvent extracts (ASE) and in supercritical fluid extracts (SFE) of the white mulberry root bark. Overall, the SFE extracts were shown to contain up to 20% Diels-Alder-type adducts, whereas in the ASE extracts a total content of more than 30% was obtained. Further SFE extracts were prepared using food grade solvents such as ethanol-water mixtures in different ratios. However, the aim of obtaining an even higher sanggenon enrichment could not be achieved (total sanggenon content >20%).

In the second research project, tissue analyses of an orally applied specialized ASE extract (MAC130LS) highly enriched in mulberry Diels-Alder-type adducts, were carried out using an UHPLC/DAD-ESI-MS/MS system. An extraction protocol for the two major constituents [**2**] and [**7**] using methanolic precipitation (-70°C, incubated for 2 h in total) was developed and validated. Finally, to confirm the presence of [**2**] and [**7**] in tissue samples (liver, lung and spleen), a comparison with the fragmentation patterns of the pure substances by MS/MS was performed.

To summarize, the analytical results show that the oral bioavailability of a white mulberry root bark extract containing 30% Diels-Alder-type adducts, is insufficient for reaching an antiviral effect. Further research on alternative application routes with respect to the best antiviral and antibacterial efficacy is subject of future studies.

ZUSAMMENFASSUNG

Das Influenzvirus ist weltweit für zahlreiche schwere Atemwegserkrankungen und Todesfälle jedes Jahr verantwortlich. Im Falle einer Sekundärinfektion, z. B. mit *Streptococcus pneumoniae*, führt der Synergismus von Virus und Bakterien zu schweren gesundheitlichen Komplikationen. Daher könnte ein dualer Mechanismus, der sowohl antivirale als auch antibakterielle Eigenschaften aufweist, die Morbiditäts- und Mortalitätsrate senken. Prenylierte Flavonoide, insbesondere die in der Wurzelrinde von *Morus alba* L. enthaltenen komplexen Diels-Alder-Addukte, haben sich in *in vitro* Studien als duale Inhibitoren erwiesen und sind vielversprechende Kandidaten, um den tödlichen Synergismus von Influenzavirus und *S. pneumoniae* auch *in vivo* zu unterbrechen.

Die vorliegende Masterarbeit befasst sich mit zwei Projekten. Das erste Projekt konzentriert sich auf die Quantifizierung von Diels-Alder-Addukten, insbesondere Kuwanon L_{130A} [**1**], Sanggenon D [**2**], Sanggenon B [**3**], Sanggenon G [**4**], Sanggenon O [**5**], Sanggenon E [**6**], Sanggenon C [**7**] mit Hilfe der Ultra-Hochleistungsflüssig-Chromatographie (UPLC) in Spezialextrakten der weißen Maulbeerwurzelrinde, die mittels „accelerated solvent extraction“ (ASE) oder mit überkritischen Lösungsmitteln (SFE) hergestellt wurden. Insgesamt wurde gezeigt, dass die SFE Extrakte bis zu 20% Diels-Alder-Addukte enthalten, während in ASE Extrakten ein Gesamtgehalt von mehr als 30% erreicht wurde. Weitere SFE Extrakte wurden mit lebensmittelgeeigneten Lösungsmitteln wie Ethanol-Wasser-Gemischen in unterschiedlichen Verhältnissen hergestellt. Hierbei konnte der Sanggenongehalt aber nicht weiter als bis ca 20% gesteigert werden.

Im zweiten Projekt wurden Gewebeanalysen eines oral verabreichten ASE Spezialextrakts (MAC130LS), der stark mit Diels-Alder-Addukten aus der Maulbeere angereichert ist, mit einem UHPLC/DAD-ESI-MS/MS-System durchgeführt. Ein Extraktionsprotokoll für die beiden Hauptbestandteile [**2**] und [**7**] mittels methanolischer Fällung (-70°C, insgesamt 2 Stunden Inkubation) wurde entwickelt und validiert. Um das Vorhandensein von [**2**] und [**7**] in Gewebeproben (Leber, Lunge und Milz) zu bestätigen, wurde ein Vergleich mit den Fragmentierungsmustern der Reinsubstanzen mittels MS/MS durchgeführt.

Zusammenfassend zeigen die analytischen Ergebnisse, dass die orale Bioverfügbarkeit des weißen Maulbeerbaumwurzelrindenextraktes, der 30% Diels-Alder-Addukte enthält, zu gering für eine ausreichende antivirale Wirkung ist. Weitere Untersuchungen zu

alternativen Applikationswegen im Hinblick auf die beste antivirale und antibakterielle Wirksamkeit sind Thema zukünftiger Studien.

1 AIM OF THE WORK

The root bark of *Morus alba* L. is rich in prenylated flavonoids, especially Diels-Alder-type adducts, which have an antiviral and antibacterial effect. Owing to similarity of the neuraminidases (NAs) of influenza virus and *Streptococcus pneumoniae* some of the constituents of white mulberry root bark extract revealed as a promising source for natural anti-influenza virus and anti-pneumococcal substances (Grienke et al., 2016).
The aim of the first project within this work was the quantification of Diels-Alder-type adducts in white mulberry root bark extracts generated in previous experiments. Additionally, an extract optimization with biocompatible solvents (ethanol/water) was performed via supercritical fluid extraction (SFE) to maximize the content of Diels-Alder adducts. The goal was to obtain a content of this compound class of more than 20%.

The biological effect of natural substances is usually investigated in *in vitro* studies and clinical evidence for *in vivo* efficacy is often lacking. The combination of *in vitro* and *in vivo* experiments is a significant step towards meaningful results (Langeder et al., 2020).
Thus, the second project aimed to quantify selected constituents in different tissues of mice after an oral administration of white mulberry root bark extract (MAC130LS, 30% total sanggenon content). The aim of this project was to determine whether the major constituents [**2**] and [**7**] accumulate in the liver, lung and spleen by means of UHPLC/DAD-ESI-MS/MS system. Based on these results, the oral bioavailability of mulberry Diels-Alder-type adducts in mice shall be assessed.

2 INTRODUCTION

2.1 *MORUS SP.* – DISTRIBUTION AND USAGE

Mulberry is part of the genus *Morus* and belongs to plant family Moraceae. The taxonomy of *Morus* species is disputed because of its wide geographical distribution, but according to Zeng (2015) the classification of the genus *Morus* should be devided into eight species (Zeng et al., 2015). Best known among them are *Morus alba* L. (white mulberry), *Morus nigra* L. (black mulberry) and *Morus rubra* L. (red mulberry) (D'Urso et al., 2019). Plants of the Moraceae family are native in China and also widely spread in Korea and Japan, nowadays also cultivated in Europe and America.

Morus sp. plants are used as traditional medicine, but also appreciated as fruits, animal feed and landscaping. The main use of their leaves is the feed of silk worms. The silkworms depend on the leaves as food for their cocoons and silk production (Figure 1). The fruits are processed into juices, jams, liqueurs and mulberry preserves. Further, wood chips of the mulberry tree are used as pulp for paper production and as nutrient media for mushroom culture (Chan et al, 2016.; Wei et al., 2016).

Figure 1: Silkworm cocoon on mulberry leaf

Many traditional medicines comprise mulberry fruits, leaves, roots, twigs and bark due to their health benefits and treatment of illness by antimicrobial and antiviral as well as antioxidant, antidiabetic, cytotoxic and anticancer, antihyperlipidemic and neuroprotective activities (Chen et al., 2021).

2.2 *MORUS ALBA* L. – PLANT DESCRIPTION

M. alba is a deciduous and fast-growing tree, which can reach a height up to 20 m. The leaves are alternate and glossy green. The size and shape of the mulberry leaves vary from 5.0-7.5 cm. A cordate base, serrated margins and acuminate at the apex are characteristic for leaves of *M. alba*. Further, the petioles are slender and long (Figure 2). The bark looks dark grey-brown. Depending on climate zones the mulberry trees are separate male and female plants (dioecious) or have female and male flowers on the same plant

(monoecious). The flowers appear greenish and as pendulous cylindrical catkins in April until May in China. Contingent on their species, they ripen into white, red or black mulberry fruits during May to August (Chan et al., 2016 ; Zafar et al., 2013).

Figure 2: Morus alba L.

2.3 *MORUS ALBA* L. – PLANT PARTS

The white mulberry is widely spread since 659 A.D. in the traditional Chinese medicine (TCM) and the list of Chinese pharmacopoeia includes the leaves (Sang Ye), fruits (Sang Shen), twigs (Sang Zhi) and root bark (Sang Bai Pi) of *M. alba* as a constituent in medicinal preparations (Zafar et al., 2013).

The white mulberry leaves, **Sang Ye**, have various medicinal properties due to different harvest times. After frost, old leaves (Dong Sang Ye) dried in the shade are considered best for clearing severe cold symptoms. For cooling and clearing heat in the liver and brightening the eyes, the young and tender spring leaves are used. The standard Sang Ye are harvested in the late fall and should be yellowish green, undamaged and without leaf stalks for good quality (jadeinstitute.com, 2019). Additionally, the leaves of the white mulberry are expectorant and decreed as a treatment for coughs in China. Further they are applied to treat symptoms like sore throats, headaches, dizziness and vertigo.

The ripe fruits of the white mulberry, **Sang Shen**, are harvested and then dried in the sun or prepared to products of fresh berries. The fruit juice has a strengthening and cleansing effect, which is why it is used as gargle and mouthwash. Also, the fruits are said to slow down the greying of hair and are indicated for dizziness, insomnia, tinnitus, impaired vision, urinary incontinence, hypertension and diabetes (Singh et al., 2013).

The twigs of the white mulberry, **Sang Zhi**, are collected in late spring or early summer and after clearance from leaves they are dried in the sun (Zhu, 1998). They are anti-rheumatic, antispasmodic, diuretic and hypotensive (Singh et al., 2013).

The main focus in this work is on the root bark of the white mulberry also called **Sang Bai Pi** (Figure 3). The root bark is expected to be collected between late autumn and early spring. The fresh roots are freed from the brown layer by a copper knife. Importantly, the surface juice may not be discarded. Afterwards, the white root barks are dried or fried in honey. A white colour, thickness and flexibility characterise good quality of Sang Bai Pi. In TCM the root bark traditionally applied for treatment of lung heat, cough, yellow sputum, bronchitis, nephritis, oliguria and oedema (Wei et al., 2016).

Figure 3: Sang Bai Pi

2.4 *M. ALBA* ROOT BARK – BIOACTIVE COMPOUNDS

There are various compounds including flavonoids, Diels-Alder-type adducts, benzofurans, stilbene, triterpenoids and coumarins, that exhibit a wide range of biological properties, which were identified after decades of research. Bioactive compounds of the mulberry root bark have anti-inflammatory, antioxidative, antimicrobic, antidiabetic, antitumor and other pharmacological effects. Despite the known action of many identified compounds, there a still enough unexplored modes of action of Sang Bai Pi, which offers a great opportunity for further research (Wei et al., 2016).

The mulberry root bark as well as the leaves, fruits and twigs are a rich source of **flavonoids**, especially carrying a prenyl or geranyl moiety (Wei et al., 2016). One example is Sanggenol A (Figure 4): it was shown to possess anti-influenza and anti-pneumococcal activity through the ability to inhibit viral and bacterial neuraminidases (NA). A disruption of the synergism between influenza A virus and pneumococcal NA was observed *in vitro* and therefore renders the root bark a promising candidate to treat super-infection by influenza A virus and pneumococci (Grienke et al., 2016).

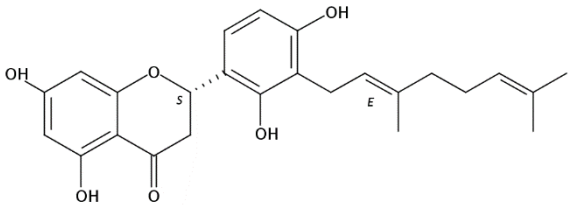

Figure 4: Sanggenol A

The most representative compounds in the white mulberry root bark are **Diels-Alder-type adducts**. They are generated by the formation of a new methylcyclohexene ring after a Diels-Alder reaction (Figure 5). The reaction occurs between a α, β-olefinic moiety of a chalcone and an isoprene unit (Yang et al., 2014).

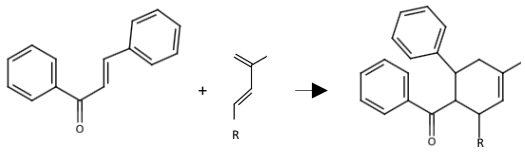

Figure 5: Diels-Alder reaction

The Diels-Alder-type adducts sanggenon C and sanggenon D account for major constituents in the root bark of *M. alba*. Due to their steric configuration, differences in the antioxidative effect were shown. In terms of reported bioactivities, such as anti-cancer, anti-inflammatory and cytoprotective effects, Sanggenon C seems more active than sanggenon D (Li et al., 2018). Furthermore, sanggenon G (Figure 6) inhibits the activity of the NA of influenza virus and pneumococci. Also, the planktonic growth and biofilm formation of *S. pneumoniae* are inhibited by sanggenon G in contrast to the known NA inhibitor oseltamivir which was not able to do so (Grienke et al., 2016). Additionally, sanggenon G supposed to be antidepressant due to interaction with the serotonergic system (Wen et al., 2019).

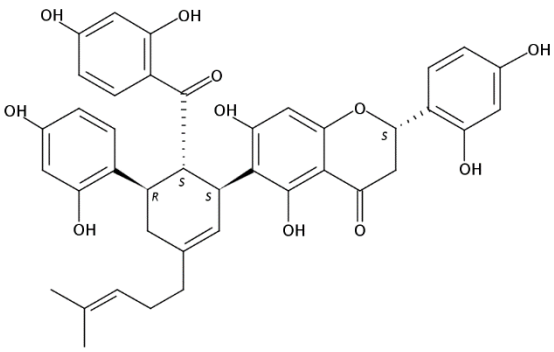

Figure 6: Sanggenon G

Further constituents isolated from the white mulberry root bark are **benzofuran-type stilbenes**, e.g. moracin O (Figure 7) and moracin P. Both show considerable neuroprotective properties against glutamate-induced cell death and notably inhibit the acetic acid-induced pain. Especially in case of neurodegenerative disorders like Parkinson's disease, Alzheimer's disease and epilepsy, glutamate and its receptor play a major role (Wang et al., 2017).

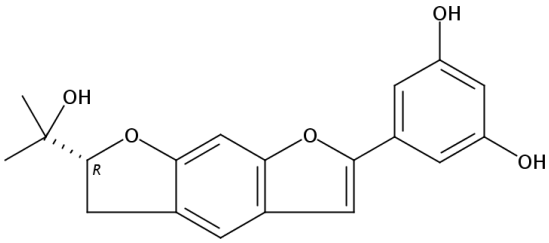

Figure 7: Moracin O

Based on a study from Cao (2018) another substance was isolated from the root bark of *M. alba*. Morescoumarin A (Figure 8), a **furocoumarin** that shows antioxidative as well as cardioprotective effects against doxorubicin-induced cell death, caused by treatment of tumours including breast cancer and soft tissue sarcomas with doxorubicin (Cao et al., 2018).

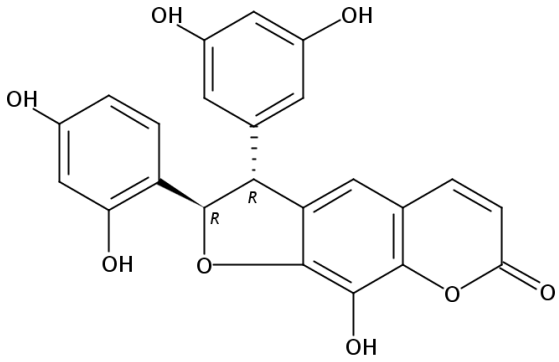

Figure 8: Morescoumarin A

The rather rare-occurring substance class of **triterpenes** in the white mulberry root bark include for example ursolic acid (Figure 9). It has reported anti-proliferative activities in different cancer cell types and therefore the potential of developments for preventive or therapeutic agents (Song et al., 2021).

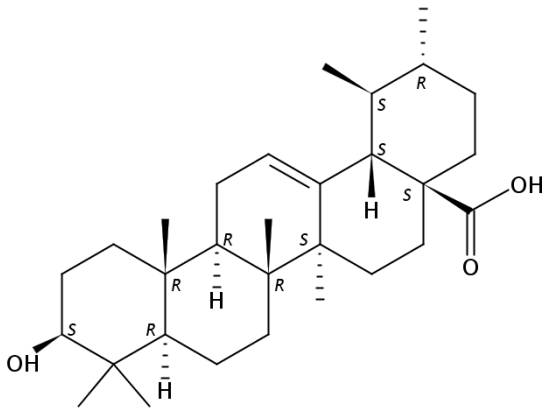

Figure 9: Ursolic acid

2.5 INFLUENZA VIRUS

In general, influenza is a seasonal disease caused by four types of seasonal influenza viruses (Type A, B, C, D) and leads to an acute respiratory infection. So far, only influenza type A virus have caused a pandemic. Due to different amino acid sequences of the surface proteins hemagglutinin (HA) and NA, the influenza A virus is further classified into subtypes. These two proteins are important targets in the antiviral therapy (e.g., NA inhibitor oseltamivir).

The circulation of seasonal influenza occurs in all parts of the world and rapidly spreads in the population, especially in confined spaces. Contagion occurs via droplet infection through sneezing, coughing or shaking hands. Therefore, special attention should be paid

to hygiene measures such as regular hand washing and covering mouth and nose with a tissue when coughing during an influenza season. In temperate climate zones the seasonal epidemic tends to be more common in winter, in tropical regions influenza is seasonal all year round, but with more irregular outbreaks.

Sudden onset of fever, cough, muscle and joint pain, headache, feeling unwell, sore throat and a runny nose are characteristic symptoms of an influenza infection. The symptoms usually subside after one week, but the virus can also cause serious illness, hospitalization and even death, especially in high-risk patients such as pregnant women, elderly, chronically ill people, children under 59 months and people with immunosuppressive conditions. Worldwide the influenza virus is estimated to be responsible for 3 to 5 million cases of severe illness and in addition about 290,000 to 650,000 respiratory deaths, annually.

Vaccination is the most effective way to prevent the severity of the disease or even infection. Annual immunisation is recommended to maintain protection and is particularly important for people at high risk and their fellow human beings in order to reduce the complications and the number of deaths caused by influenza virus (WHO, 2018).

2.6 PNEUMOCOCCI

S. pneumoniae, also called pneumococcus, is a gram-positive bacterium and globally leads to numerous severe pneumonia and pneumonia-related deaths (Morimura et al., 2021). The bacteria frequently and asymptomatically settle in the nasopharynx, especially in children. Invasive spread can cause otitis media, sinusitis, meningitis and sepsis. Young children, elderly and immune-compromised people are among the most vulnerable population group of these infections. In these populations the morbidity and mortality for severe pneumococcal disease is the highest. Outbreaks occur mainly in kindergartens and homes for elderly and homeless, and predominantly on the African meningitis belt. A major problem in the treatment of pneumococci is the increasing resistance to commonly used antibiotics, such as penicillin, macrolides, cephalosporins and co-trimoxazole (Morimura et al., 2021; WHO, 2018). Since 2017 *S. pneumoniae* is on the list of antibiotic-resistant priority pathogens of the World Health Organisation (WHO) because of its main

human health danger (WHO, 2017). Hence, effective vaccines and advanced therapeutics, such as herbal medicine, is still of utmost importance.

2.7 SYNERGISM OF INFLUENZA VIRUS AND PNEUMOCOCCI

Infection with influenza virus is often associated with secondary infection of pneumococci. This co-pathogenesis increases the severity of the disease and mortality rate (Walther et al., 2016). This lethal synergism of influenza virus and *S. pneumoniae* is mediated by NAs, which are presented on both pathogens. There is a perfect interplay between the viral NAs, which provides important receptors sites and growth-promoting nutrients for the bacteria, and the bacterial NAs, which have supportive function in viral release. Due to the similarity of the viral and bacterial NAs a dual inhibition of both NAs is expected to be beneficial for therapy leading to a decrease in mortality. Hence, the focus has been on the identification of new substances with NA-inhibitory potential from plant sources in recent years, as there are currently few efficient drugs on the market.

The bioactive compounds from *M. alba* deserve increasing attention as source for anti-infectives. As mentioned in studies, especially the compounds sanggenon G and sanggenol A show inhibition of viral and bacterial NAs *in vitro*. This gives the opportunity for further research in an *in vivo* setting for the disruption of the lethal synergism of influenza virus and pneumococci (Grienke et al., 2016).

2.8 *IN VIVO* EXPERIMENT

The essential basis of this Master thesis is formed by two previous diploma theses, one previous Master thesis and an *in vivo* experiment. Firstly, Freisinger (2020) dealt with the optimization of processing white mulberry root bark extracts and the preparative separation of prenylated compounds (Freisinger, 2020). Secondly, the isolation and enrichment of its compounds on large scale was carried out by Rumpold (Rumpold, 2020). Lastly, Jahoda (2022) worked on the isolation and purification of these constituents of the white mulberry root bark as well as their quantification in different extracts (Jahoda, 2022).

Confirmations of the dual inhibition of NAs of *M. alba* compounds *in vitro*, finally prompted *in vivo* experiments with MAC130LS. The latter is a specialized *M. alba* root bark extract produced in previous studies by means of ASE. The extract was optimized to a maximized enrichment in mulberry Diels-Alder-type adducts that exert dual inhibition of influenza virus and *S. pneumoniae* (Grienke et al., 2016; Jahoda, 2022).

Female BALB/c mice, weighing approximately 20 g, were used to study the tolerability, anti-influenza activity and distribution of the constituents of the extract MAC130LS in plasma and tissue samples after oral application. The extract was administered orally by gavage to the mice in a dose finding study with doses of 30 mg/kg, 100 mg/kg, 300 mg/kg bodyweight (n=20). In a subsequent infection trial, animals were treated with the 100 mg per kg bodyweight dose (n=46). The mice in the dose finding study were sacrificed three hours after administration. In the infection trial, four mice from each group (mock treated and verum group) were sacrificed one hour and the remaining four mice from both groups 24 hours after the last extract administration. Plasma, liver, spleen and lung were resected, weighted in fresh state and stored at -70°C until the analysis. An overview of the *in vivo* experiment is given in Table 9 (page 29).

3 PROJECT 1:

ANALYSIS OF WHITE MULBERRY ROOT BARK EXTRACTS

3.1 MATERIALS AND METHODS

In this section, the used materials, instruments, reagents and methods as well as their settings are listed and explained.

3.1.1 Materials, reagents and instruments

The root bark from *M. alba* for the SFE extracts prepared during this thesis (batch no 820797) and the already existing ASE and SFE extracts (batch no. 460797) was purchased from Plantasia in 2020 and 2018, respectively. Voucher specimens (2021: JR-20200221, 2018: JR-20190928-A1) are deposited at the Department of Pharmaceutical Sciences, Division of Pharmacognosy, University of Vienna, Austria. The existent ASE extracts were abbreviated with MAC1** and the designation MAC0** was utilized for SFE extracts.
All solvents and instruments used for this project are presented in Table 1 and Table 2.

Table 1: Used solvents and reagents

Solvent/reagent	**Specifications**	**Usage**
Acetone	ÖAB distilled	for SFE
Acetonitrile	HiPerSolv CHROMANORM® ≥99.9%	for UPLC
CO_2	Messer CO_2 4.5	for SFE
Ethanol	Brenntag Austria GmbH ÖAB distilled	for SFE
Isopropanol	AnalaR NORMAPUR 100%	for SFE
Methanol	HiPerSolv CHROMANORM® ≥99.9%	for UPLC
Water	Double distilled	for SFE

Table 2: Used instruments

Instrument	Description
Centrifuge	Minispin, Eppendorf
Rotary evaporator	R-210, Büchi Laboratorium Technologie AG
SFE	Waters MV-10 Software: ChromScope 1.6
Ultrasonic Bath	Transsonic T 469, Elma
UPLC	Waters Acquity UPLC H-Class Modules: PDA, ELSD Software: Empower 3
Vacuum pump	V-710, Büchi
Vortex mixer	Heidolph REAX 200

3.1.2 Supercritical fluid extraction

Supercritical fluid extractions (SFE) were carried out by using a Waters MV-10 SFE device. It is composed of a fluid delivery module cooled down by a chiller to 4°C, a 10-vessel column oven adjusted at 40°C, an automated backpressure regulator, a heat exchanger and an extraction collector. The software ChromScope 1.6 was used. The vessels for extraction had a volume of 5 ml, respectively. For extractions, 1.0 g of powdered white mulberry root bark was placed in the extraction vessel and filled up with glass beads. Sub/supercritical CO_2 was used as solvent A and different experiments with isopropanol (IPA), acetone and several ethanol-water mixtures (EtOH/H_2O: 50/50; 60/40; 70/30; 80/20; 90/10) were utilized as co-solvent (solvent B). The designation of the extracts with the respective solvents can be found in Table 3 .The method for extraction had already been developed and optimized in previous preliminary experiments. The settings are presented in Table 4. The obtained extracts were transferred into a round bottom flask and evaporated to dryness in the rotavapor. For complete dryness the extracts were kept in a desiccator overnight.

Table 3: Designation of the extracts with their used co-solvents

Sample	Co-Solvent
MAC062	IPA
MAC063	acetone
MAC060	50% EtOH/50% H_2O
MAC064	60% EtOH/40% H_2O
MAC065	70% EtOH/30% H_2O
MAC066	80% EtOH/20% H_2O
MAC067	90% EtOH/10% H_2O

Table 4: Optimised methods for SFE

Sample name	MAC060		MAC062 - MAC067	
	Defatting step	Extraction step	Defatting step	Extraction step
Oven temperature °C	40	40	40	40
Pressure (bar)	300	200	300	200
Flow rate (ml/min)	10	10	10	10
Solvent A (ml)	10	8	10	7
Solvent B (ml)	0	2	0	3
Make up – ethanol (ml)	2	0	2	0
Dynamic 1 (min)	5	2	5	2
Static (min)	5	2	5	2
Dynamic 2 (min)	5	2	5	2
Cycles	1	3	1	3

3.1.3 Ultra-performance liquid chromatography (UPLC)

For quantification of mulberry extracts, a chromatographic method was developed. The optimization with regard to the selection of the stationary phase, mobile phase compositions, run time, sample volume and wave length was carried out by Jahoda et. al. (2022). The analyses were implemented on a Waters ACQUITY H-class UPLC system which is composed of an automatic sample manager adjusted to 8°C, a quaternary solvent manager, a column manager, a photodiode array detector (PDA) and an evaporative light scattering detector (ELSD). For the separation of the compounds a mobile phase consisting of water (solvent A) and acetonitrile (ACN) (solvent B) was utilized. The mobile phase was pushed through an ACQUITY UPLC BEH Phenyl column (1.7 µm, 2.1×100 mm,)

kept at 40°C with a flow rate of 0.3 ml/min and a total run time of 10 min, followed by an equilibration time of 5 min. The gradient program [T(min)/%B] was 0/5; 1/50; 6.9/50; 7/98; 8.9/98; 9/5; 10/5. A volume of 1 µl for each sample was injected (Empower: dilution factor 5) and the wave length of detection was set at 205 nm. The data acquisition and processing were executed by Waters Empower 3 software.

The method of quantification was established and validated according to the International Council for Harmonisation of Technical Requirements for Pharmaceuticals for Human Use (ICH) guidelines by Jahoda et. al. (2022). Using this method, the quantification of the compounds in the extracts, kuwanon L_{130A} [**1**], sanggenon D [**2**], sanggenon B [**3**], sanggenon G [**4**], sanggenon O [**5**], sanggenon E [**6**], sanggenon C [**7**] was implemented.

In Figure 10, the chromatogram of MAC131 with assigned constituents [**1**]-[**7**] is shown.

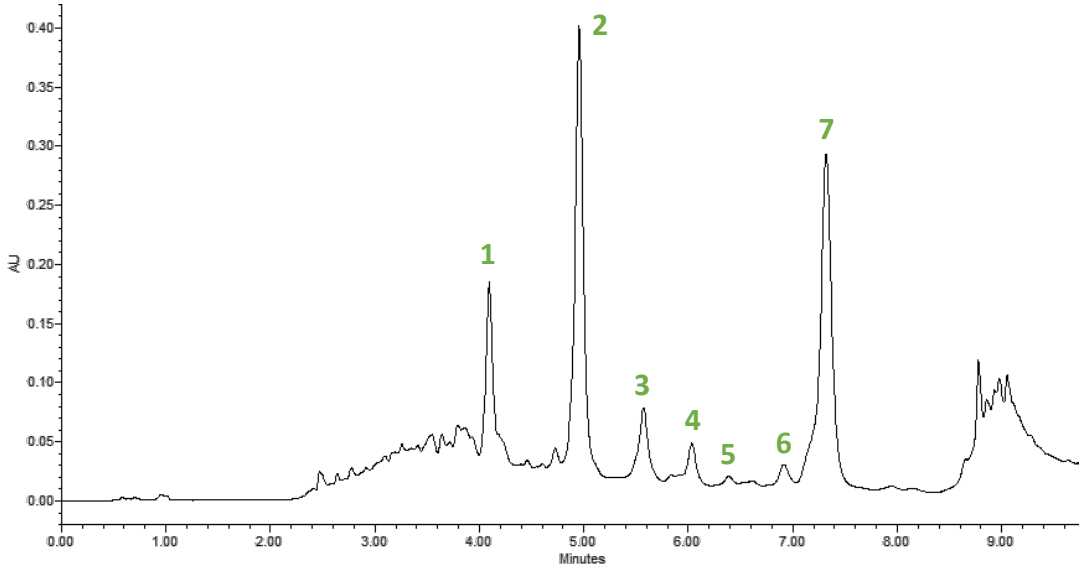

Figure 10: UPLC chromatogram of MAC131 at 205 nm (PDA)

3.1.4 Preparation of samples

Before sample preparation, all ASE and SFE extracts were stored in a desiccator for complete desiccation. 1.0 – 1.5 mg of the respective extracts were transferred into 1.5 ml Eppendorf tubes and dissolved in 1 ml HPLC-grade methanol and subsequently ultrasonicated. For the sample preparation of the herein produced SFE extracts approximately 2.5 – 3.0 mg were dissolved in 1 mL HPLC-grade methanol. For a better dissolving, extracts were treated in an ultrasonic bath for 5 min, followed by vortexing.

After centrifuging the samples for 5 min with 13,400 rpm, the supernatant was transferred in vials and placed into the automatic sample manager for the measurement via the H-class UPLC system.

3.2 RESULTS

3.2.1 Quantification of ASE extracts

In previous experiments, different accelerated solvent extracts (ASE) were produced using a variety of different extraction settings and extraction solvents. To determine the composition of the compounds [**1**-**7**] in the extracts, they were analysed by UPLC. Samples were prepared according to the preparation protocol in Materials and methods (page 20) and measured in triplicates. The quantifications were performed as described by Jahoda et al. (2022). The obtained results are presented in Table 5 and Table 6.

The results indicate that extract MAC131 has the highest overall content of mulberry Diels-Alder-type adducts closely followed by the extract MAC129. Both show an enrichment in these prenylated flavonoids above 30% in total. In contrast to that, in the extracts MAC118, MAC119, MAC122 and MAC123 no measurable amounts of **1**-**7** were found.

*Table 5: Quantification of compounds **1-7** in ASE-extracts*

sample	Kuwanon L_{130A} [1] [%]	Sanggenon D [2] [%]	Sanggenon B [3] [%]	Sanggenon G [4] [%]	Sanggenon O [5] [%]	Sanggenon E [6] [%]	Sanggenon C [7] [%]	sum identified [%]
MAC101	2.23	3.51	0.09	0.15	0.09	0.33	2.53	**8.92**
MAC102	1.44	2.77	n.f.	0.06	0.11	0.30	2.10	**6.79**
MAC103	1.80	1.84	0.04	n.f.	0.08	0.21	1.90	**5.87**
MAC104	0.89	1.59	n.f.	0.04	0.08	0.32	1.52	**4.45**
MAC105	4.18	4.06	0.27	0.05	0.09	0.27	3.25	**12.17**
MAC106	4.54	6.63	0.47	0.45	0.13	0.47	4.68	**17.37**
MAC107	2.46	3.84	0.12	0.15	0.18	0.34	2.74	**9.83**
MAC108	2.23	4.02	0.16	0.25	0.17	0.35	2.87	**10.05**
MAC109	0.98	0.22	n.f.	0.09	0.24	n.f.	n.f.	**1.52**
MAC110	1.28	2.21	n.f.	0.07	0.11	0.29	1.67	**5.63**
MAC111	1.54	2.87	0.05	0.15	0.17	0.32	2.06	**7.16**
MAC112	6.48	11.23	1.17	7.56	0.25	0.71	7.56	**28.34**
MAC113	1.82	3.01	0.04	0.15	0.12	0.35	2.14	**7.64**
MAC114	1.47	2.93	0.02	0.16	0.14	0.35	2.13	**7.20**
MAC115	1.53	3.19	0.04	0.19	0.15	0.38	2.44	**7.92**
MAC116	1.27	0.28	0.13	n.f.	0.12	0.27	1.22	**3.29**

n.f. … not found

*Table 6: Quantification of compounds **1-7** in ASE-extracts*

sample	Kuwanon L_{130A} [1] [%]	Sanggenon D [2] [%]	Sanggenon B [3] [%]	Sanggenon G [4] [%]	Sanggenon O [5] [%]	Sanggenon E [6] [%]	Sanggenon C [7] [%]	sum identified [%]
MAC117	2.57	5.42	n.f.	0.42	0.13	0.22	2.80	**11.55**
MAC118	n.f.	n.f.	n.f.	n.f.	n.f.	n.f.	n.f.	**n.f.**
MAC119	n.f.	n.f.	n.f.	n.f.	n.f.	n.f.	n.f.	**n.f.**
MAC120	5.13	8.97	0.99	0.54	0.27	0.53	6.07	**22.50**
MAC121	4.19	8.12	0.77	0.62	0.27	0.62	5.89	**20.49**
MAC122	n.f.	n.f.	n.f.	n.f.	n.f.	n.f.	n.f.	**n.f.**
MAC123	n.f.	n.f.	n.f.	n.f.	n.f.	n.f.	n.f.	**n.f.**
MAC124	5.45	10.72	0.76	0.90	0.33	0.82	8.10	**27.08**
MAC125	5.03	10.58	1.13	1.13	0.53	1.01	7.07	**26.47**
MAC126	5.92	11.48	1.17	0.85	0.28	0.73	8.24	**28.67**
MAC127	5.31	9.48	0.80	0.66	0.26	0.68	7.77	**24.97**
MAC128	2.70	4.56	0.21	0.29	0.12	0.42	3.47	**11.76**
MAC129	6.72	11.62	1.56	0.99	0.34	0.70	8.72	**30.65**
MAC131	6.35	11.78	1.44	1.09	0.33	0.85	9.71	**31.54**
MAC132	5.89	8.67	1.07	1.09	0.30	0.65	7.23	**24.88**
MAC133	5.55	9.16	0.84	0.75	0.30	0.79	7.83	**25.23**

n.f. … not found

3.2.2 Quantification of SFE extracts

SFE extracts previously prepared under varying extraction conditions were prepared for the analysis by UPLC according to the established protocol. All SFE extracts were analysed in triplicates and quantitated by the same method as the ASE extracts. The obtained results of the previously prepared SFE extracts are shown in Table 7 (page 27).

Additional to the existing SFE-extracts, further extracts were produced. Through the SFE-based extract optimization, the aim was to get the highest possible enrichment of sanggenons.

SFE extracts were prepared with supercritical CO^2 and IPA and acetone as co-solvents (co-solvents reaching a maximum of 30%), because these extraction co-solvents previously resulted in the highest sanggenon contents. Furthermore, several ethanol-water mixtures (Table 3) were tested as co-solvents with the aim to obtain a biocompatible extract with a total amount of more than 20% mulberry Diels-Alder-type adducts. The obtained results of the sanggenon quantification of the newly manufactured SFE extracts are listed in Table 8 (page 28).

Considering the results of the extractions with the co-solvents IPA and acetone a high enrichment of compounds [**1**-**7**] was achieved (IPA: 36.60%; acetone: 45.93%) underlining the good extraction properties of IPA and acetone for the targeted compounds. Significantly high amounts were observed for the main components [**2**] and [**7**]. The other compounds [**1** and **3**-**6**] showed significantly lower contents. In comparison with the extracts generated with ethanol-water mixtures as co-solvents, IPA and acetone resulted in notably higher amounts of mulberry Diels-Alder adducts.

When comparing the total sanggenon amounts of the extracts derived from ethanol-water co-solvent mixtures, the results show a noticeable increase only for extracts generated with an ethanol content of 80% of the co-solvent (Table 8). Analysis of the different sanggenons in MAC060, MA0C64, and MAC065 resulted in a comparable composition even though the ethanol content increased by 10%, respectively. [**2**] and [**7**] showed to be the main components with the highest values also in these extracts. The extraction settings of MAC066 revealed a two-fold increase in total sanggenon content,

compared to the extracts prepared with a lower ethanol content as a co-solvent. By an increase of the ethanol content from 80% to 90% of the co-solvent, the sanggenon content increased by >5%.
Despite satisfactory result of the extract MAC067, the aim of getting a sanggenon content of >20% could not be achieved with an extraction using ethanol-water mixtures as co-solvent.

Comparing the results of the total amount of the most enriched and promising ASE and SFE extracts, the ASE extracts are superior to existing SFE extracts in a magnitude of a 10% higher content in sanggenons in total. Also, several ASE extracts achieved more than 20% overall content whereas all SFE extracts were lower. However, the SFE extracts prepared within this thesis with isopropanol and acetone resulted in sanggenon contents up to 45%. This leads to the conclusion that both ASE and SFE are suitable methods for the extraction of the target components.

*Table 7: Quantification of compounds **1-7** in SFE-extracts*

sample	Kuwanon L_{130A} [1] [%]	Sanggenon D [2] [%]	Sanggenon B [3] [%]	Sanggenon G [4] [%]	Sanggenon O [5] [%]	Sanggenon E [6] [%]	Sanggenon C [7] [%]	sum identified [%]
MAC010	1.43	1.22	0.09	0.05	n.f.	0.15	1.19	**4.12**
MAC019	1.51	1.49	n.f.	n.f.	0.08	0.19	1.42	**4.66**
MAC030	1.70	1.91	n.f.	n.f.	0.08	0.18	1.99	**5.87**
MAC033	1.03	0.80	n.f.	n.f.	0.11	0.19	1.71	**3.85**
MAC036	3.02	4.30	0.26	0.11	0.10	0.27	3.49	**11.54**
MAC039	3.61	5.17	0.57	0.28	0.16	0.35	4.24	**14.39**
MAC041	3.91	5.98	0.43	0.21	0.12	0.30	6.17	**17.12**
MAC042	n.f.	n.f.	n.f.	n.f.	n.f.	n.f.	n.f.	**n.f.**
MAC043	1.93	2.91	0.05	0.07	0.09	0.21	3.24	**8.51**
MAC044	1.00	1.04	0.15	n.f.	0.10	n.f.	1.38	**3.66**
MAC045	2.63	3.80	n.f.	0.18	0.11	0.26	2.88	**9.85**
MAC046	1.14	1.59	0.05	0.05	0.07	0.18	1.49	**4.56**
MAC049	4.20	6.06	0.64	0.34	0.21	0.33	4.37	**16.15**
MAC051	4.42	7.37	0.83	0.55	0.25	0.46	6.01	**19.89**
MAC053	3.87	5.17	0.51	0.38	0.19	0.36	4.08	**14.56**
MAC055	3.22	5.78	0.28	0.27	0.15	0.34	6.69	**16.73**
MAC057	1.53	2.05	n.f.	0.04	n.f.	0.18	1.50	**5.31**

n.f. … not found

*Table 8: Quantification of compounds **1-7** in newly prepared SFE-extracts*

sample	Co-Solvent	Kuwanon L_{130A} [1] [%]	Sanggenon D [2] [%]	Sanggenon B [3] [%]	Sanggenon G [4] [%]	Sanggenon O [5] [%]	Sanggenon E [6] [%]	Sanggenon C [7] [%]	sum identified [%]
MAC062	IPA	2.20	14.03	1.71	0.33	0.81	2.46	15.07	**36.60**
MAC063	acetone	2.61	15.71	1.42	0.37	0.66	3.99	21.17	**45.93**
MAC060	50% EtOH/50% H_2O	0.41	3.07	0.24	0.02	0.07	0.44	2.80	**7.04**
MAC064	60% EtOH/40% H_2O	0.39	2.47	0.21	n.f.	0.10	0.48	2.69	**6.34**
MAC065	70% EtOH/30% H_2O	0.58	2.39	0.18	0.06	0.11	0.46	2.67	**6.44**
MAC066	80% EtOH/20% H_2O	1.05	5.55	0.60	0.13	0.16	0.85	5.02	**13.37**
MAC067	90% EtOH/10% H_2O	1.74	6.92	0.96	0.33	0.25	1.15	7.11	**18.47**

n.f. … not found

4 PROJECT 2: ANALYSIS OF TISSUE SAMPLES

4.1 MATERIALS AND METHODS

In this section, all details of the materials, reagents, instruments and methods used for the experiments as well as their settings are listed and explained.

4.1.1 Tissue samples, reagents and instruments

The tissue samples of the *in vivo* experiments which are shown in Table 9, were applied for analysis. All solvents and instruments used for this project are listed in Table 10 and Table 11.

Table 9: Overview of in vivo experiment

Study type	**Treatment**	**Sample number** (Liver, spleen, lung)
Blank	-	524 525
Dose finding (Sacrificed after 3 h; n=20)	**30 mg/kg**	526 527 528 529 530
	100 mg/kg	531 532 533 534 535
	300 mg/kg	536 537 538 539 540
Infection trial (100 mg/kg; n=46)	**mock treated** (Sacrificed after 1 h)	541 542 543 544 545 546 547 548
	treated (Sacrificed after 1 h)	564 565 566 567
	treated (Sacrificed after 24 h)	568 569 570 571

Table 10: Used solvents and reagents

Solvent/reagent	Specifications	Usage
Acetonitrile	HiPerSolv CHROMANORM® ≥99.9%	for LC-MS/MS
Formic acid	ROTIPURAN® ≥98%	for LC-MS/MS
Methanol	HiPerSolv CHROMANORM® ≥99.9%	for homogenate, spike solution, methods
Water	Double distilled	for LC-MS/MS, homogenate

Table 11: Used instruments

Instrument	Description
Centrifuge	Minispin, Eppendorf Centrifuge 5424 R, Eppendorf Zentrimix 380 R
Evaporator	GeneVac EZ-2 plus
Ultrasonic Bath	Transsonic T 469, Elma
UPLC/DAD-ESI-MS/MS	Dionex UltiMate 3000 LC Modules: LTQ XL ion trapp mass spectrometer, DAD Xcalibur software
Vortex mixer	Heidolph REAX 200

4.1.2 LC-MS/MS conditions

The UHPLC/DAD-ESI-MS/MS system was composed of a Dionex UltiMate 3000 LC system coupled to an LTQ XL ion trap mass spectrometer. The system was equipped with a photo diode array detector (DAD), a pump, an autosampler adjusted to 4°C and a column oven. The chromatographic separation was achieved on a Waters Acquity BEH Phenyl column (1.7 µm, 1.2×100 mm) and the column was kept at room temperature. The flow rate was 0.3 ml/min, and the injection volume was set to 5 µl. The mobile phase consisted of 0.1% formic acid aqueous solution (A) and 0.1% formic acid acetonitrile solution (B). The gradient elution was set as follows: [T(min)/%B] 0/30, 5/50, 10/80, 15/98. Data acquisition, processing and the analyte concentration calculations were determined using Xcalibur software.

4.1.3 Method development

Several methods for sample preparation were tested to quantitatively measure [**2**] and [**7**] in the biological tissue samples. Experiments with different solvents and varying incubation times were carried out to find the most suitable method with a maximum extraction recovery of the two standards. An overview of the different methods is shown in Table 12.

Table 12: Parameters leveraged during establishment of a sample preparation protocol

Protocol #	**Solvent for homogenate**	**Solvent for extraction** (Cooled at -70°C)	**Incubation time**
1	MeOH	MeOH	4 h; 1h
2	MeOH	MeOH ACN + 1% formic acid	1 h; 30 min
3	MeOH	MeOH	1h; 30 min; 30 min
4	ddH_20	MeOH	1h; 30 min; 30 min

4.1.3.1 Sample preparation protocol 1

Figure 11: Mouse liver

A mock treated liver (sample 523) (Figure 11) served as blank tissue. After removal from storage (-70°C), it was thawed before use and then cut. 1,500 µl methanol (cooled to -70°C) and zirconium beads were added to the blank liver in a 2.0 ml tube. The liver was homogenized in the Zentrimix 380R at 4°C for 7 min at 1,500 rpm. All further processing steps of the liver homogenate were performed on ice. A spike solution of MAC130LS with a concentration of 1.10 mg/ml in methanol was prepared. First, 100 µl of the liver homogenate (poorly pipettable) were spiked with 10 µl spike solution and shortly vortexed. Then 500 µl methanol (-70°C) were added. Subsequently, the sample was vortexed and incubated for 4 h at -70°C. After incubation, the sample was centrifuged at 15,000 rpm for 10 min using a refrigerated centrifuge (4°C). Then the supernatant was transferred to a new Eppendorf tube and stored (on ice) until the next step. 400 µl methanol (cooled to -70°C) were added to the precipitate, which was

vortexed for 1 min and then incubated for another 30 min at -70°C. Afterwards, the sample was centrifuged at 15,000 rpm for 10 min using a refrigerated centrifuge (4°C) again. The supernatant was transferred and combined from both extractions. The supernatant was dried in the GeneVac EZ-2 plus with the programme ´Aqueous´ at 30°C. After bringing to complete dryness, the pellet was stored at -70°C until analysis.

4.1.3.2 Sample preparation protocol 2

For further optimization, the same liver homogenate and spike solution was used as in protocol 1. Likewise, the further processing was performed on ice. First, two tubes with 50 µl of the liver homogenate were spiked with 10 µl spike solution and shortly vortexed. Then in one tube 500 µl of acetonitrile containing 1% formic acid solution (cooled at -70°C) and in the other tube 500 µl methanol (cooled at -70°C) were added. The samples were put into the ultrasonic bath for 5 min and were also shortly vortexed. This was followed by incubation at -70°C for 1 h. Thereafter, the tubes were centrifuged at 15,000 rpm for 10 min using a refrigerated centrifuge (4°C). The supernatants of each sample were transferred and stored in new Eppendorf tubes. 400 µl of the afore used solvent (acetonitrile with 1% formic acid, or methanol) were added to the samples and vortexed following by incubation for 30 min at -70°C. Furthermore, the tubes were centrifuged at the same conditions in the refrigerated centrifuge like before. The supernatants were transferred and combined with the stored ones. They were put into the GeneVac EZ-2 plus and were completely dried with the programme ´Aqueous´ at 30°C. The dried pellets were stored at -70°C until further processing.

4.1.3.3 Sample preparation protocol 3

In this method the liver homogenate and the spike solution are the same as in protocol 1. Also, the further processing was performed on ice. 50 µl homogenate was spiked with 10 µl spike solution. After vortexing, 500 µl methanol (cooled at -70°C) were added to the homogenate followed by a 5 min ultrasonication and shortly vortexing. The sample was incubated for 1 h at -70°C. In the next step the sample was centrifuged for 10 min at 15,000 rpm in a refrigerated centrifuge (4°C) and the supernatant was transferred in a new Eppendorf tube. The step was repeated two more times, but with 400 µl methanol and an incubation time of 30 min. The supernatants from the incubation steps were

combined and were dried in the GeneVac EZ 2-plus with ´Aqueous´ at 30°C. The dried pellet was stored at -70°C until the preparation for LC-MS measurement.

4.1.3.4 Sample preparation protocol 4

The preparation of tissue homogenates was performed with blank samples from the liver (524), the lung (523) (Figure 12) and the spleen (523) (Figure 13). The frozen tissues were thawed before use and then cut. The sliced tissues were given in separate tubes. 500 µl double-distilled water (ddH_2O) and zirconium balls were added, respectively. In the Zentrimix 380R (4°C) the samples were crushed for 15 min at 1,500 rpm to a homogenate. The same spike solution as in protocol 1 was used. Further processing of each tissue homogenate was performed according to protocol 3.

Figure 12: Mouse lung

4.1.4 Optimized tissue sample extraction protocol

All tissue samples were separately homogenized according to the presented sample preparation protocol 4. However, in the case of liver due to a volume limited to 2 ml, not the whole organ was used but only about 200 mg. 900 µl methanol (cooled at -70°C) were added to the tissue homogenates. The mixtures were put into an ultrasonic bath for 5 min and shortly vortexed followed by incubation for 1.5 h at -70°C. Afterwards, the samples were centrifuged for 10 min at 15,000 rpm in a refrigerated centrifuge (4°C). The supernatants were transferred to new Eppendorf tubes. 400 µl of fresh methanol (cooled at -70°C) were added to precipitations. Subsequently, the samples were ultrasonicated for 10 min before vortexing. Then incubation for 30 min at -70°C was performed. This was followed by centrifugation again. The supernatants were transferred, combined and finally dried in the GeneVac EZ 2-plus. The dried pellets were stored at -70°C until UPLC/DAD-ESI-MS/MS measurement.

Figure 13: Mouse spleen

For the analysis of the extracted tissue samples, the dried pellet was dissolved in 50 µl of HPLC-grade methanol. The Eppendorf tubes were vortexed on the upper and lower side. Then the sample was put into the ultrasonic bath for 5 min and subsequently centrifuged

for 5 min at 13,400 rpm. The supernatant was transferred into HPLC vial inserts for UHPLC/DAD-ESI-MS/MS measurements.

4.1.5 Method validation

The optimized UHPLC/DAD-ESI-MS/MS method for analysis of tissue samples from the *in vivo* study was validated in accordance with ICH guidelines (ICH, 1995) for its specificity, linearity, precision and recovery. The validation parameters are presented in Table 15 (page 38).

First, a dilution series of two standards, namely sanggenon D [**2**] and sanggenon C [**7**] isolated and purified by Rumpold (2020), for preparation of calibration curves and the determination of the linearity range were used (Figure 14, Figure 15). A stock solution in a concentration of approximately 1 mg/ml (level 0) for both standards in methanol was prepared. The stock solutions were serially diluted in a ratio of 1:3 for 11 further calibration levels. Each level was injected in triplicate and the integration of the peaks were carried out with Xcalibur software (Quan browser).

The calibration curves of the standards [**2**] and [**7**] exhibited a good linearity over the tested concentration ranges, level 3 – level 12. LOD and LOQ values were defined visually as the concentration of the signal-to-noise-ratio of at least 3 and 10 times, respectively.

Precision was evaluated by intraday (evaluation within 1 day) and interday (evaluation over 3 days) experiments for [**7**]. The intraday parameter was conducted with four measurements of sample 564-liver, due to shortness of sample volume. For interday experiments the sample 565-liver was used.

The MS/MS mode was used to evaluate the identity of [**2**] and [**7**] in the tissue samples. Fragmentation patterns of the MS/MS spectra of the standards were compared with those of selected tissue samples. The spectra are shown in chapter Results (page 46) and Appendix (page 58 ff).

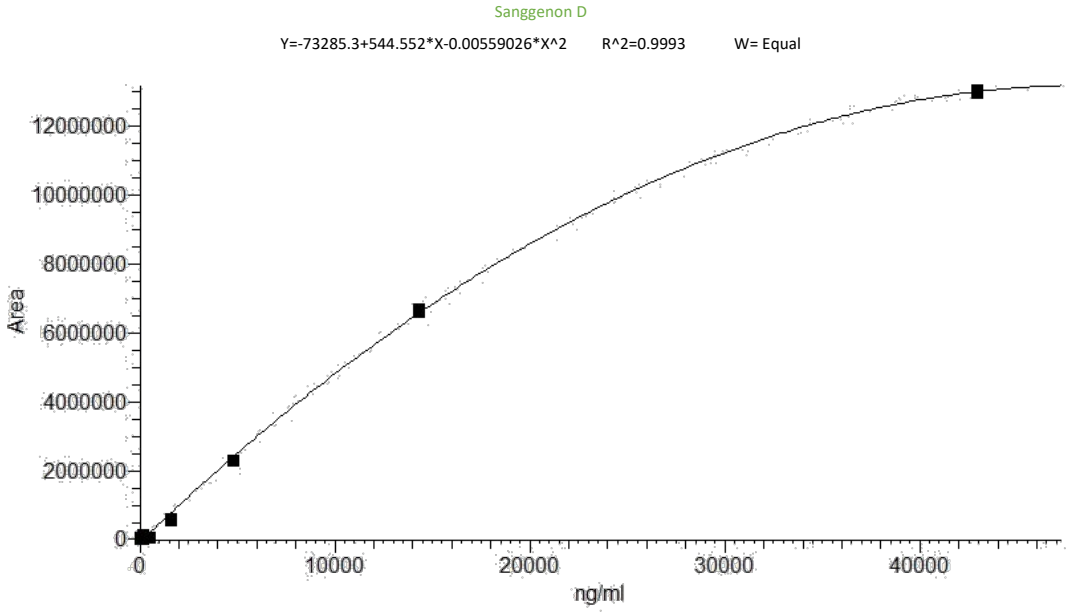

*Figure 14: Calibration curve for sanggenon D [**2**]*

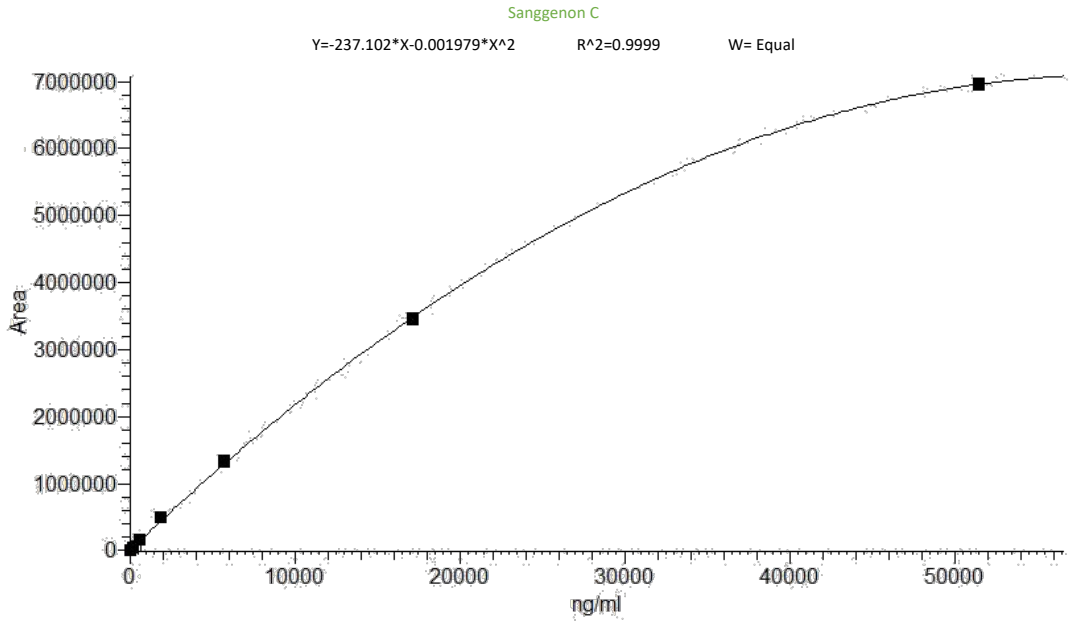

*Figure 15: Calibration curve for sanggenon C [**7**]*

4.2 RESULTS

4.2.1 Development of an extraction protocol for tissue samples

The dried pellets of the several methods were prepared for UHPLC/DAD-ESI-MS/MS measurements and subsequently measured using the optimized method listed in chapter Materials and methods (page 31). The aim was to find a method with an extraction recovery rate of more than 70% of the two compounds [**2**] and [**7**], respectively. However, the main focus was rather on [**2**]. When evaluating the results, it was immediately obvious that the extraction of [**7**] was not comparably successful. For the calculation of the recovery rate, the peak areas of the negative mode from the measured samples and spike solution were defined, respectively. Afterwards, the recovery rate of [**2**] and [**7**] in the tissue samples was expressed in % in comparison to the spike solution. The extraction recovery rates of tissues for the respective protocols are shown in Table 13.

Table 13: Extraction recoveries of tissues for each protocol (Protocol 1-3 mixed with MeOH, 4 mixed with ddH_2O)

Protocol #	**Sanggenon D [2]** AUC neg mode [%]	**Sanggenon C [7]** AUC neg mode [%]
liver		
1	57	12
2 (methanol)	80	27
2 (acetonitrile)	63	14
3	85	26
4	74	33
spleen		
3	82	70
4	84	73
lung		
3	60	52
4	72	54

First, the extraction recovery of [**2**] and [**7**] in protocol 1 was far below the desired value. Compared to other methods, the incubation time was much longer. In protocol 2-4 the first incubation periods were rigorously shortened from 4 h to 1 h and interestingly, this led to significantly better recovery rates of [**2**] and [**7**].

Secondly, in protocol 2 a comparison of the extraction solvents methanol and ACN + 1% formic acid was carried out. The ACN + 1% formic acid solution turned out to be a poor solvent for tissue extraction. The extraction recovery rate with methanol as solvent was considerably higher.

Due to a repeated number of incubation periods from two to three in protocol 3 and 4, improvements in the extraction recovery rates of [**2**] (60% - 85%) and [**7**] (26% - 73%) were achieved compared to the other methods again.

In protocol 4, the solvent for the preparation of homogenates was changed from methanol to ddH_2O. The processing of homogenates with ddH_2O and the pipettability were better reproducible, compared to the homogenate with methanol. Likewise, the colour was more reddish and did not appear denatured. Table 14 shows the results of protocols 3 and 4 from the different tissues for comparison. Protocol 4 attained higher recovery rates of [**2**] and [**7**] from lung and liver, though a lower recovery rate of [**2**] from liver compared to protocol 3. However, the results from protocol 4 were acceptable, due to the use of ddH_2O and was therefore considered as the optimized tissue extraction protocol for preparation of homogenates.

Table 14: Extraction recoveries of protocol 3 (MeOH) and protocol 4 (ddH_2O)

	tissue	MeOH	ddH_2O
sanggenon D [2] AUC neg mode [%]	liver	85	74
	spleen	82	84
	lung	60	72
sanggenon C [7] AUC neg mode [%]	liver	26	33
	spleen	70	73
	lung	52	54

4.2.2 Method validation

Due to a triplicate injection of the standards [**2**] and [**7**] in serial dilution with increasing concentrations quadratic calibration curves were received. The linearity range of [**2**] was determined from 2.1 ng/ml to 42 962 ng/ml and of [**7**] from 2.62 ng/ml to 51 481.48 ng/ml. Additionally, a good correlation for both standards is shown (correlation coefficient for [**2**]: R^2= 0.9993; [**7**]: R^2= 0.9999).

LOD was visually detected as at least 3 times the concentration of the signal-to-noise ratio and amount 3.92 ng/ml for [**2**] and 4.71 ng/ml for [**7**]. LOQ was defined at least 10 times the concentration of the signal-to-noise ratio and was determined as 13.05 ng/ml for [**2**] and 15.70 ng/ml for [**7**].

Precision was specified as the deviation of absolute peak areas within one day (intraday) using liver sample 564 and over three days (interday) expressed in %. Liver sample 565 was used and determined only for precision of [**7**]. The standard deviation for intraday was generated from four injections instead of six, due to shortness of sample. Precision values for the presented method range from 6.2% of intraday and 7.71% of interday analyses.

The extraction recovery of the several methods is listed in Table 13 (page 36). Results show an extraction recovery for [**2**] from 72% to 84% and for [**7**] from 33% to73% using water for homogenization in dependence on the used tissue (liver, lung or spleen). All validation parameters are listed in Table 15.

Table 15: Results of method validation

Compounds	**Sanggenon D [2]**	**Sanggenon C [7]**
Regression equation (y)	-73285.3+544.552*X-0.00559026*X^2	237.102*X-0.001979*X^2
Correlation coefficient (R^2)	0.9993	0.9999
Linearity range (ng/ml)	2.1 – 42 962	2.62 – 51 481.48
LOD (ng/ml)	3.92	4.71
LOQ (ng/ml)	13.05	15.70
Precision (%)		
Intraday	n.d.	6.20
Interday	n.d.	7.71
Extraction recovery (%)	72-84	33-73

4.2.3 Analysis of tissue samples

By means of an *in vivo* experiment in mice, we aimed to investigate the distribution of compounds [**2**] and [**7**] contained in the MAC130LS extract in the tissues after oral administration. An overview of the different types of treatment and sample numbers in the *in vivo* study is shown in Table 9 (page 29).

Different tissue samples such as liver, lung and spleen were prepared in accordance with the optimized extraction protocol for tissue samples, which can be seen in chapter Materials and methods (page 33). All samples were measured in duplicate by UHPLC/DAD-ESI-MS/MS. The quantification was based on the average value of the peak areas of the two technical replicates and values were calculated by the means of calibration curves of [**2**] and [**7**]. As already mentioned in Materials and methods (page 33), only a part of the liver was used for extraction. For the determination of the effective extraction rate of [**2**] and [**7**] from liver, the obtained extraction rate was computed to the total weight of liver. Due to the complex sample matrix, a comparably high signal-to-noise ratio was observed in the measurements of the tissue samples, especially in the case of liver samples. The blank or mock-treated samples of the experiment showed a high signal-to-noise ratio in each tissue type. Therefore, the LOD and LOQ had to be increased to obtain the actual extraction rates. To calculate the real extraction rate, the highest measured average noise value of blank or mock-treated samples of the respective tissues was subtracted from average values of the corresponding samples from the same tissue type. The concentrations of [**2**] and [**7**] in each tissue sample are listed in Table 16 (page 41) and are graphically represented in Figure 16 and Figure 17.

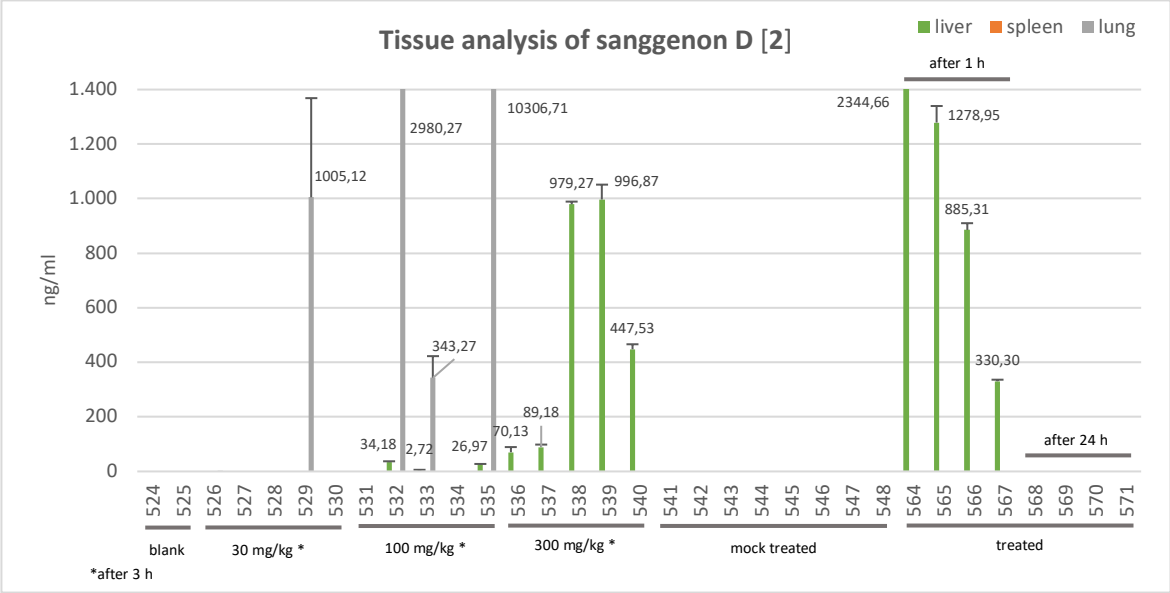

*Figure 16: Results of tissue analysis of sanggenon D [**2**]*

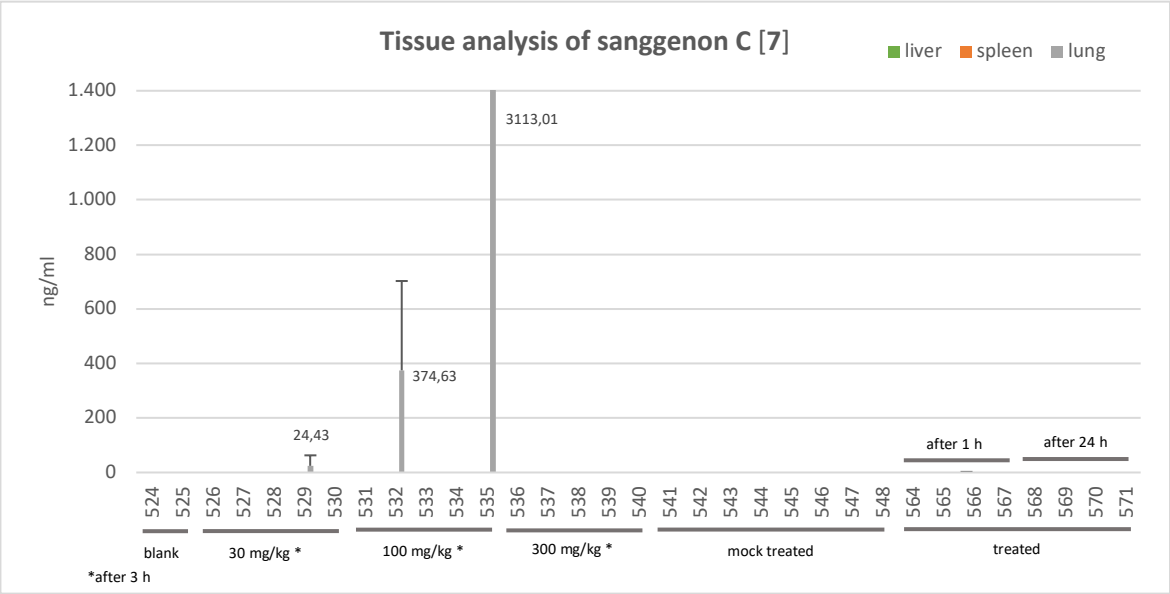

*Figure 17: Results of tissue analysis of sanggenon C [**7**]*

Table 16: Results of tissue analysis

	sample	Sanggenon D [2] (ng/ml)			Sanggenon C [7] (ng/ml)		
		liver	**spleen**	**lung**	**liver**	**spleen**	**lung**
Dose finding	**524**	n.f.	n.f.	n.f.	n.f.	n.f.	n.f.
	525	n.f.	n.f.	n.f.	n.f.	n.f.	n.f.
	526	n.f.	n.f.	**1.73** (± 60.98)	n.f.	n.f.	n.f.
	527	n.f.	n.f.	n.f.	n.f.	n.f.	n.f.
	528	n.f.	n.f.	n.f.	n.f.	n.f.	n.f.
	529	n.f.	n.f.	**1,005.12** (± 363.45)	n.f.	n.f.	**24.43** (± 38.45)
	530	n.f.	n.f.	n.f.	n.f.	n.f.	n.f.
	531	n.f.	n.f.	n.f.	n.f.	n.f.	n.f.
	532	**34.18** (± 3.01)	n.f.	**2,980.27** (± 676.59)	n.f.	n.f.	**374.63** (± 327.67)
	533	**2.72** (± 3.22)	n.f.	**343.27** (± 79.39)	n.f.	n.f.	n.f.
	534	n.f.	n.f.	n.f.	n.f.	n.f.	n.f.
	535	**26.97** (± 0.44)	n.f.	**10,306.71** (± 411.57)	n.f.	n.f.	**3,113.01** (± 1451.73)
	536	**70.13** (± 19.14)	n.f.	n.f.	n.f.	n.f.	n.f.
	537	**89.18** (± 9.23)	n.f.	n.f.	n.f.	n.f.	n.f.
	538	**979.27** (± 9.95)	n.f.	n.f.	n.f.	n.f.	n.f.
	539	**996.87** (± 54.59)	n.f.	n.f.	n.f.	n.f.	n.f.
	540	**447.53** (± 18.69)	n.f.	n.f.	n.f.	n.f.	n.f.
Infection trial	**541**	n.f.	n.f.	n.f.	n.f.	n.f.	n.f.
	542	n.f.	n.f.	n.f.	n.f.	n.f.	n.f.
	543	n.f.	n.f.	n.f.	n.f.	n.f.	n.f.
	544	n.f.	n.f.	n.f.	n.f.	n.f.	n.f.
	545	n.f.	n.f.	n.f.	n.f.	n.f.	n.f.
	546	n.f.	n.f.	n.f.	n.f.	n.f.	n.f.
	547	n.f.	n.f.	n.f.	n.f.	n.f.	n.f.
	548	n.f.	n.f.	n.f.	n.f.	n.f.	n.f.
	564	**2,344.66** (± 78.13)	n.f.	n.f.	n.f.	n.f.	n.f.
	565	**1,278.95** (± 60.76)	n.f.	n.f.	n.f.	n.f.	n.f.
	566	**885.31** (± 24.79)	n.f.	n.f.	**2.10** (± 0.05)	n.f.	n.f.
	567	**330.30** (± 6.01)	n.f.	n.f.	n.f.	n.f.	n.f.
	568	n.f.	n.f.	n.f.	n.f.	n.f.	n.f.
	569	n.f.	n.f.	n.f.	n.f.	n.f.	n.f.
	570	n.f.	n.f.	n.f.	n.f.	n.f.	n.f.
	571	n.f.	n.f.	n.f.	n.f.	n.f.	n.f.

Considering the results of the quantification of [**2**] in the dose finding study a noticeable difference between the types of tissues was detected. These results are shown in detail in Figure 18.

First, in none of the spleen samples compound [**2**] could be detected. This led to the conclusion, that oral administration of the extract did not cause to accumulation of compound [**2**] in spleen after 1 h, 3 h or 24 h. Secondly, the comparison of the extraction rates in lung samples showed some irregularities. On closer analysis, in lung sample 526 minimal concentration and in sample 529, 532, 535 high values of compound [**2**] were determined. A slight dose dependence between 30 mg/kg and 100 mg/kg was recognisable. But considering the values of the highest treatment dose samples of 300 mg/kg, no enrichment of [**2**] could be measured. Therefore, a dose dependence of [**2**] in the lung samples was not given. Further studies need to be conducted to study the bioaccumulation of sanggenons in lung samples in mice. One explanation for this phenomenon could be the oral application of the extract via gavage: Therein the oesophagus might have been injured in some animals, leading to high concentrations of [**2**] detected in scattered individuals (529, 532, 535).

However, comparing the values of the different doses in liver samples, a dose dependency became apparent. At the lowest dose 30 mg/kg no significant amounts of [**2**] were found. At the 100 mg/kg dose, notable concentrations of compound [**2**] were present in 3 of 5 samples. In liver sample 536-540, a significant increase of the amount of [**2**] at the highest dose was evident. This suggested a dose dependence accumulation of compound [**2**] in liver samples at 3 h after the last oral application of MAC130LS.

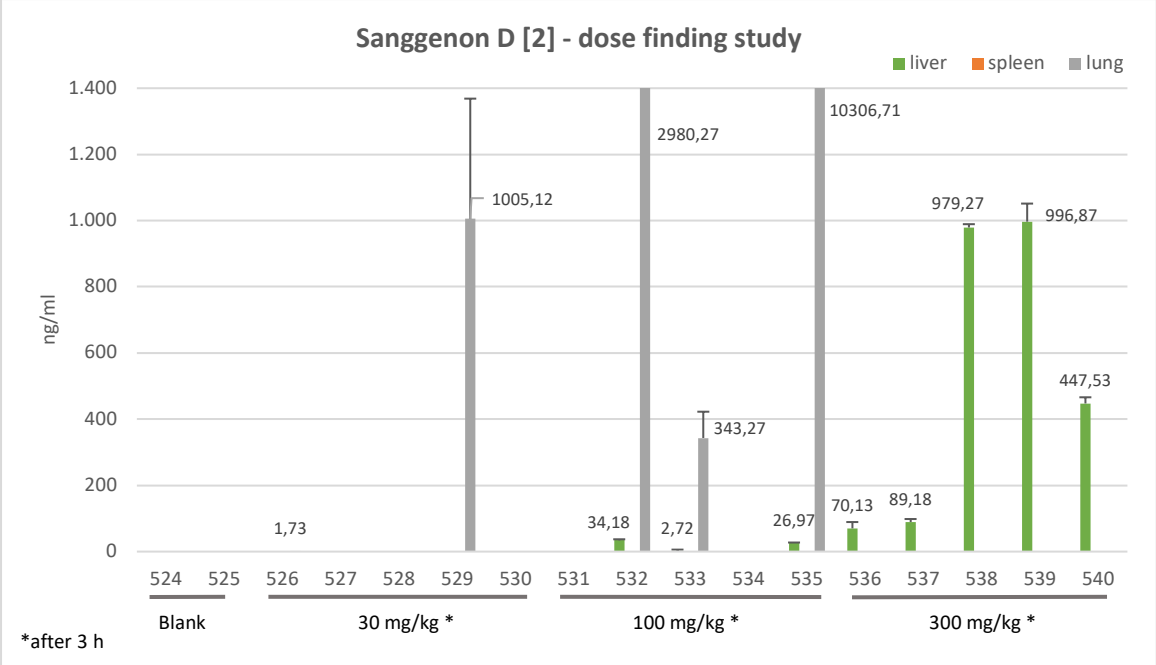

*Figure 18: Results from dose finding study of sanggenon D [**2**]*

Interesting results emerged from the quantification of [**2**] in the infection trial. These results are shown in detail in Figure 19. Neither in spleen, nor in lung measurable values of the compound were quantitated. On the contrary to these tissue types, in liver samples significant concentrations were found. The treated mice 564-567 were sacrificed 1 h after the last oral administration of the extract and these liver samples presented high quantities of [**2**]. Comparing the samples of sacrifice after 1 h (564-567) and 24 h (568-571) after the last extract application, compound [**2**] was not detectable after 24 h anymore. Concludingly, there is a rapid degradation or metabolization and no bioaccumulation was determined of compound [**2**] in the liver samples.

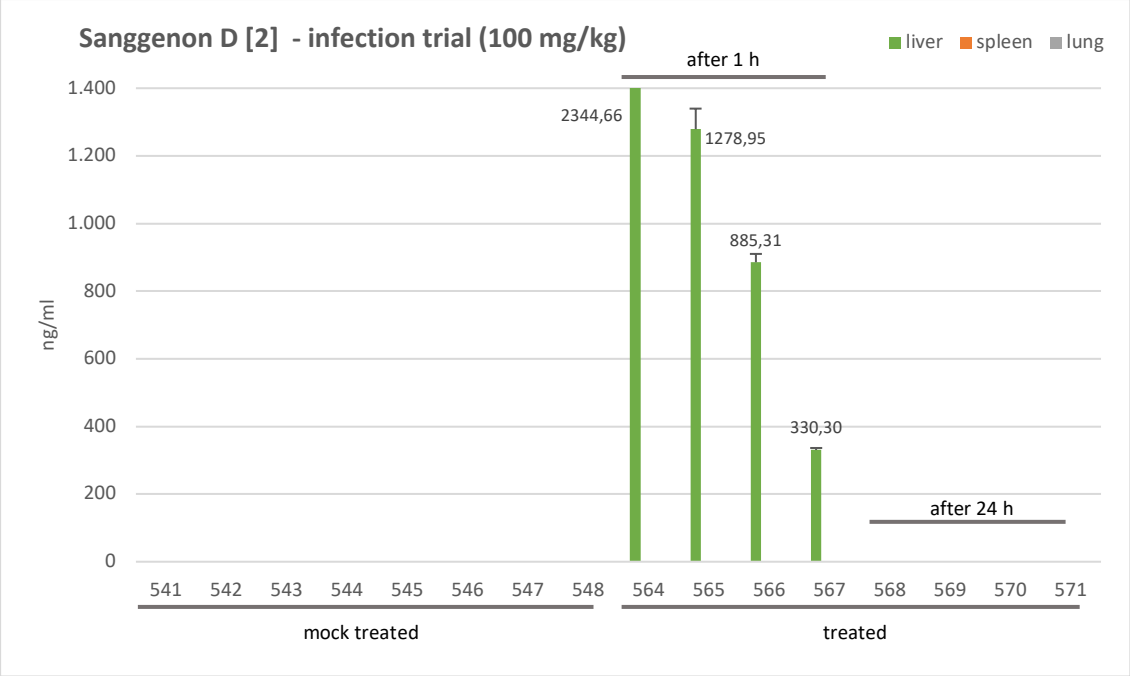

*Figure 19: Results from infection trial of sanggenon D [**2**]*

Compared to compound [**2**], the results of [**7**] are hard to interpret. The results of the dose finding study of compound [**7**] are shown in Figure 20.

Neither in liver nor in spleen samples a detectable amount of [**7**] was found in the dose finding experiment. Concerning the lung samples, at a treatment dose of 30 mg/kg minimal values in sample 529 and in the dose group of 100 mg/kg in sample 532 and 535 significant concentrations were measured. Similar results were shown in the infection trial. Only in lung sample 566 with a mouse sacrifice after 1 h a minimal concentration of compound [**7**] was determined.

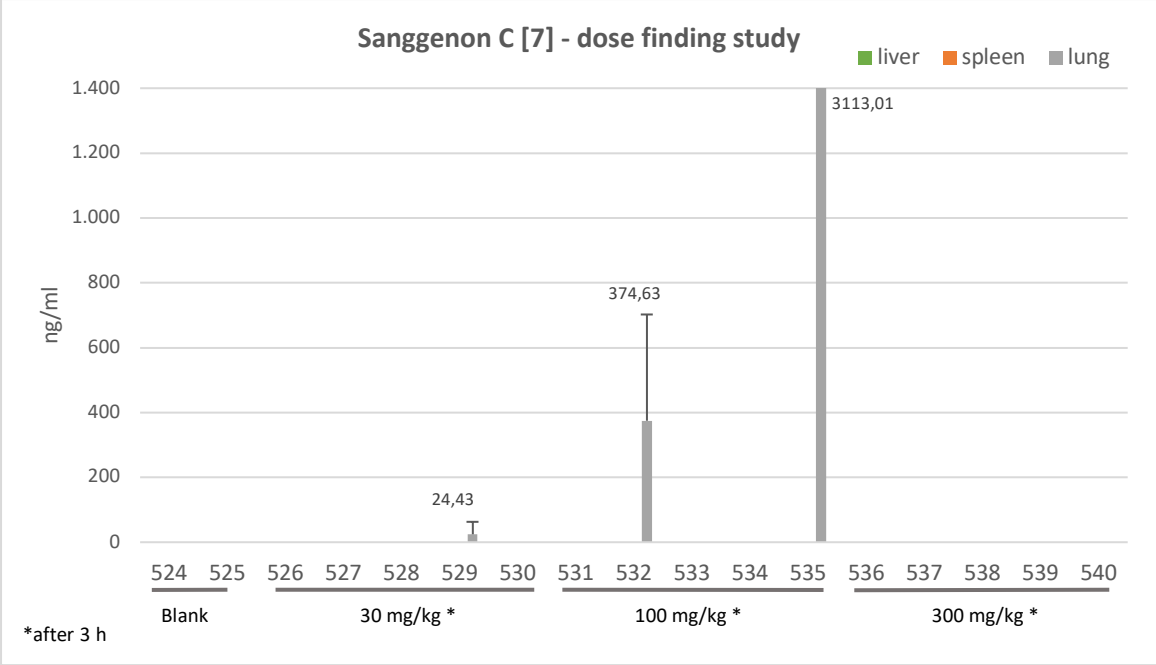

*Figure 20: Results from dose finding study of sanggenon C [**7**]*

As the results indicate, the measured values of compound [**7**] are lower in both studies compared to compound [**2**] which confirms our results during method establishment: Considering the extraction recoveries, better reliability for compound [**2**] than for [**7**] was shown, especially in liver and lung. However, both constituents were not detected in any spleen sample.

Dose dependency and rapid metabolism of [**2**] were determined in liver samples, whereas [**7**] was detected in only one sample. Furthermore, both metabolites were measured in only few lung samples. High values of [**2**] and [**7**] in sample 532 and 535 were found. Otherwise, there was little correlation in the obtained quantification result. In conclusion, there is an accumulation of [**2**] and [**7**] in liver and lung 1h and 3 h after oral administration of extract MAC130LS, but no significant amounts of neither [**2**], nor [**7**] were detected 24 h after the last application. Therefore, the results suggest that mulberry Diels-Alder-type adducts contained in MAC130LS have an oral bioavailability below 1%.

4.2.3.1 Comparison of MS/MS spectra

To confirm the specificity of the analytical method and thereby the presence of the constituents [**2**] and [**7**] in the measured tissue samples, MS/MS measurements were carried out. First, fragmentation patterns of [**2**] (Figure 21) and [**7**] (Figure 22) were defined to compare the patterns of the tissue samples in which concentrations were measured at the respective retention times. The fragmentation fingerprint of both prenylated flavonoids presented four main fragments (m/z values: 369.1; 463.2; 579.3; 638.2), which were assigned to the structure and marked in the following figures.

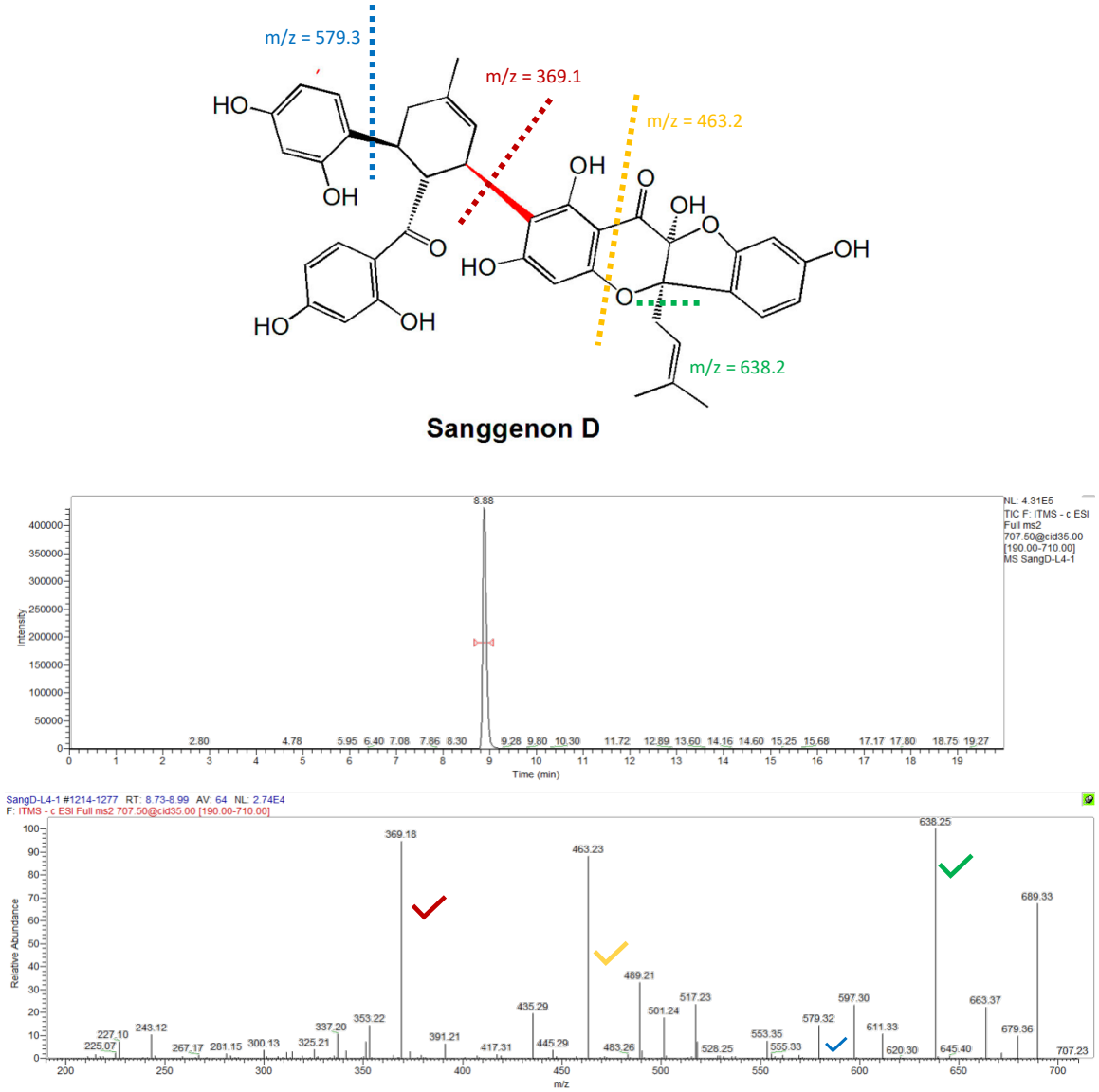

*Figure 21: Fragmentation pattern an fragments of sanggenon D [**2**]*

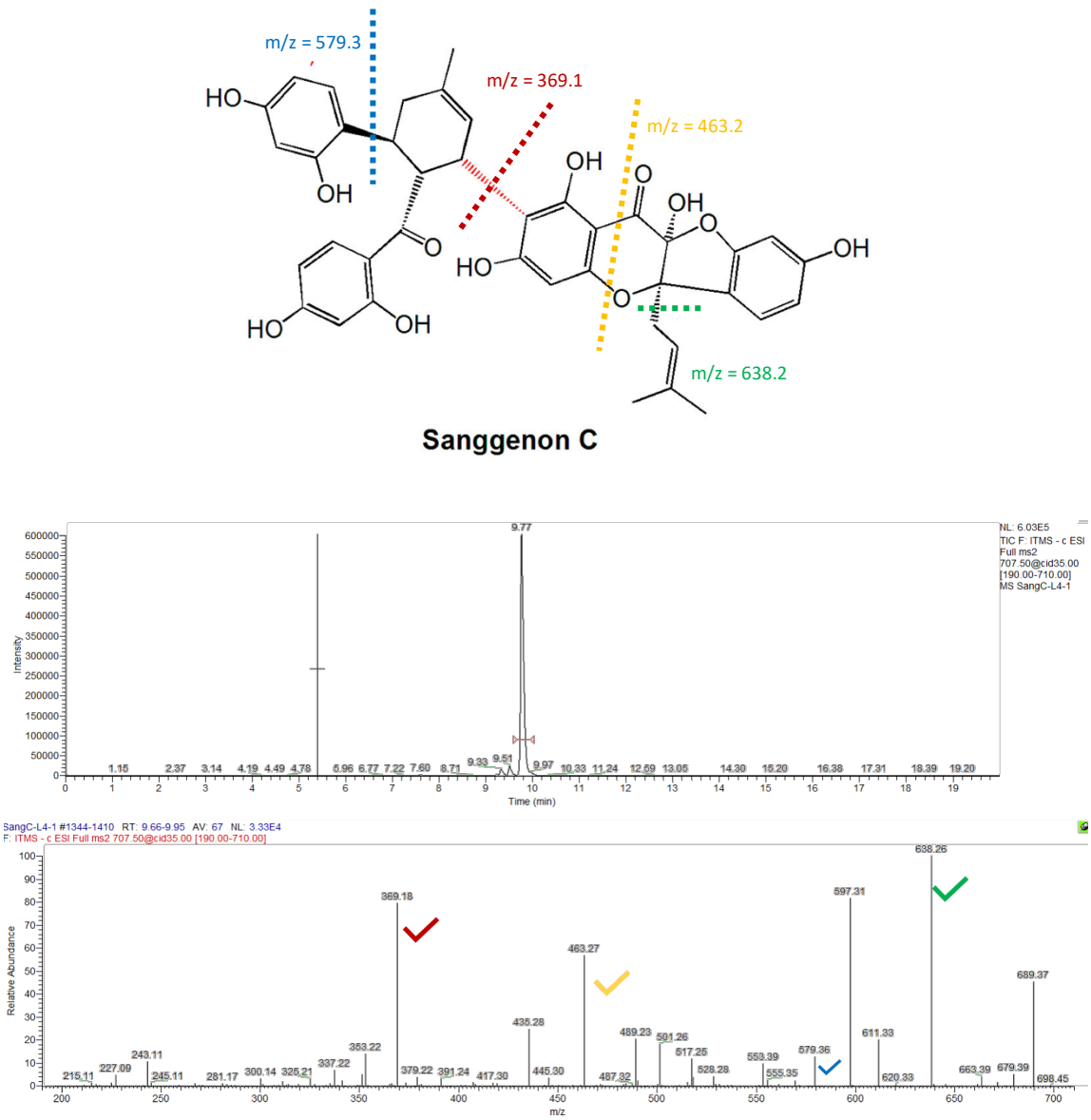

*Figure 22: Fragmentation patterns and fragments of sanggenon C [**7**]*

For tissue samples, in which significant concentrations of [**2**] and/or [**7**] were determined, the fragmentation pattern was detected using MS/MS. Table 17 shows the samples used for the fragmentation pattern comparison including confirmation of presence of [**2**] and [**7**].

*Table 17: MS/MS confirmation list of presence of [**2**] and [**7**] in analysed samples marked as **✓***

Sample numbers	Sanggenon D [2]	Sanggenon C [7]
Lung samples		
526	✓	-
529	✓	✓
532	✓	✓
533	✓	-
535	✓	✓
Liver samples		
524	-	✗
532	✓	-
533	n.d.	n.d.
535	n.d.	n.d.
536	n.d.	n.d.
537	n.d.	n.d.
538	✓	-
539	✓	-
540	✓	-
564	✓	-
565	✓	-
566	✓	✗
567	✓	-

n.d. … not determined

The fragmentation pattern of the lung samples validated the presence of [**2**] and [**7**] after comparison of fragment fingerprint of the pure substance. The same result was obtained by comparing the fragmentation patterns of liver samples. Importantly, the chromatogram of blank liver 524 showed a peak at the retention time of [**7**]. With the aid of comparing the fragmentation pattern of [**7**] and 524, no presence of the compound was determined. Thus, the peak in liver samples did not show the presence of [**7**] when no concentration was measured (Figure 23). Moreover, the fragmentation pattern of compound [**7**] in sample 566 was interesting. Due to extremely small concentration of [**7**] in this sample, no clear fragmentation pattern of [**7**] was discernible. The fragments were only present in very low intensity followed to no explicit confirmation of [**7**]. Thus, once more we herein confirm, that for the analysis of sanggenons in tissue samples, sanggenon D [**2**] is superiorly suited than sanggenon C [**7**] due to specificity and extraction recovery. Fragmentation patterns of all listed samples are shown in Appendix (page 58).

All in all, these results confirm specificity of the presented method compounds [**2**] after oral administration, especially in liver and lung samples.

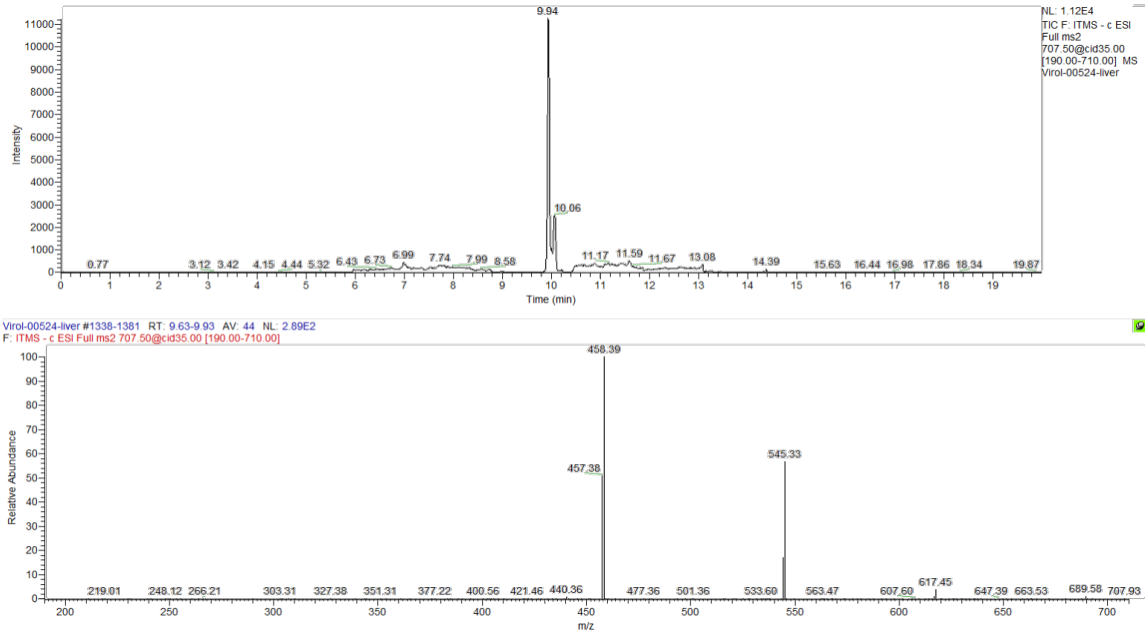

*Figure 23: Fragmentation pattern of liver sample 524 at retention time of sanggenon C [**7**]*

5 DISCUSSION AND CONCLUSION

The influenza virus is causing an epidemic and pandemic of severe acute respiratory illnesses with high morbidity and mortality rates. Co-infections with *S. pneumoniae* exacerbate the severe disease progression and further increase the death toll (Walther et al., 2016). In addition to effective vaccination, increasing attention is being paid to antiviral and antibacterial compounds from natural sources, which act on both pathogens at the same time. The root bark from the TCM plant *M. alba* was shown to simultaneously combat influenza virus and pneumococci, including an additional inhibition of biofilm formation. This renders the white mulberry root bark a promising lead in the development of therapeutics against the lethal synergism of the these two pathogens (Grienke et al., 2016). Most of the recent studies dealing with natural products focus on *in vitro* experiments. Though, in order to draw conclusions about the pharmacokinetic and pharmacodynamic effects of individual compounds, *in vivo* studies are essential. Thus, a combination of *in vitro* and *in vivo* experiments are of importance for the discovery of effective drugs from natural origin (Langeder et al., 2020).

The first project of this Master thesis deals with extracts obtained by ASE and SFE containing mulberry Diels-Alder-type adducts. Previously prepared ASE and SFE extracts of the white mulberry root bark were analysed for their sanggenon content, on the other hand the preparation and following quantification of SFE extracts with different co-solvents, such as IPA, acetone and ethanol-water mixtures in different ratios was carried out. The content of compounds [**1** - **7**] was analysed using the optimised and validated method established by Jahoda (2022). Looking at the results of ASE extracts, MAC131 (31.54%) contained the highest total amount of Diels-Alder-type adducts in white mulberry root bark followed by MAC129 (30.65%).

For the SFE extracts prepared with the co-solvents IPA and acetone high amounts of target compounds were determined (36.60% and 45.93%, resp.). Furthermore, ethanol-water mixtures in different ratios (EtOH/H_2O: 50/50; 60/40; 70/30; 80/20; 90/10) were applied as co-solvents for SFE to achieve the goal of producing biocompatible *M. alba* root bark extracts with a total content of Diels-Alder-type adducts higher than 20%. Using an extraction solvent composed of 70% supercritical CO_2 and 30% co-solvent (80% ethanol)

allowed to increase the total amount of sanggenons to >10% (MAC066). A further increase in ethanol (90%) of the co-solvent even reached a total Diels-Alder-type adduct content of 18.47% (MAC067). However, these results indicate that it is hardly possible to generate biocompatible SFE extracts with >20% sanggenons.

All in all, comparison of ASE and SFE extracts shows that both methods allow for an enrichment in bioactive mulberry Diels-Alder-type adducts to an extend of 30-45%. Further, when comparing the quantitative results of all analysed ASE and SFE extracts to previously examined traditional extracts, a six- to eleven-fold concentration even on the extract basis (Jahoda, 2022).

The second project in this Master thesis focused on tissue analysis from a previously conducted *in vivo* experiment, where mice were orally administered an ASE extract (MAC130LS; 29% total sanggenon content) in a dose finding study and an infection trial. The oral bioavailability of compound [**2**] and [**7**] and their concentration in liver, spleen and lung was investigated. For maximally efficient extraction rates of Diels-Alder-type adducts, a sample extraction protocol with -70°C methanol as precipitation agent and two incubation circles (1.5 h; 30 min) was established. The measurements of all tissue samples were carried out on a LC-MS/MS instrument. The whole quantification protocol was successfully validated.

The results of the tissue analysis showed a better reliability of [**2**] than of [**7**] in liver and lung in terms of extraction recovery and specificity. Looking at the results, a dose dependence as well as a rapid metabolism of [**2**] in the liver could be observed. Neither [**2**] nor [**7**] were detected in spleen samples. To confirm the correct identification of Diels-Alder-type adducts in the tissues with detected ions, fragmentation patterns of the reference substances [**2**] and [**7**] isolated by Rumpold (2020) were compared by LC-MS/MS. Further, both marker compounds were quantified in a few lung samples, but without conclusive informative value. This effect might be deduced from injury during extract application via gavage. Thus, further studies are required to investigate the bioaccumulation of sanggenons in lungs.

In conclusion, accumulation of [**2**] and [**7**] in liver and lung 1 h or 3 h after oral administration of extract MAC130LS was evident, but neither [**2**] nor [**7**] were detected

after 24 h after the last application. To summarize, white mulberry Diels-Alder-type adducts contained in MAC130LS have an oral bioavailability below 1%.

Further in-depth investigations like the study of alternative routes of application (e.g. intravenous or inhalative administration) might be an option in order to achieve sufficient amounts of the promising Diels-Alder-type adducts in the organism to exploit their full potential against the lethal synergism of influenza virus and *S. pneumoniae*.

REFERENCES

CABI – Invasive Species Compendium

https://www.cabi.org/isc/datasheet/34816#toPictures (Accessed: 22. February 2022).

Cao, Y., Zheng, X., Yang, F., Li, F., Qi, M., Zhang, Y., Zhao, X., Kuang, H., & Feng, W. (2018). Two new phenolic constituents from the root bark of *Morus alba* L. and their cardioprotective activity. *Natural Product Research*, *32*(4), 391–398. https://doi.org/10.1080/14786419.2017.1309535

Chan, E. W.-C., Lye, P.-Y., & Wong, S.-K. (2016). *Phytochemistry, pharmacology, and clinical trials of Morus alba*. 15.

Chen, C., Mohamad Razali, U. H., Saikim, F. H., Mahyudin, A., & Mohd Noor, N. Q. I. (2021). Morus alba L. Plant: Bioactive Compounds and Potential as a Functional Food Ingredient. *Foods*, *10*(3), 689. https://doi.org/10.3390/foods10030689

D'Urso, G., Mes, J. J., Montoro, P., Hall, R. D., & de Vos, R. C. H. (2019). Identification of Bioactive Phytochemicals in Mulberries. *Metabolites*, *10*(1), 7. https://doi.org/10.3390/metabo10010007

Freisinger, V. (2020). *Analytics and fractionation of prenylated compounds*. Diploma thesis. University of Vienna, Departement of Pharmacocgnosy. http://urn:nbn:at:at-ubw:1-26862.31068.317152-6

Grienke, U., Richter, M., Walther, E., Hoffmann, A., Kirchmair, J., Makarov, V., Nietzsche, S., Schmidtke, M., & Rollinger, J. M. (2016). Discovery of prenylated flavonoids with dual activity against influenza virus and Streptococcus pneumoniae. *Scientific Reports*, *6*(1), 27156. https://doi.org/10.1038/srep27156

ICH Guidelines: European Medicine Agency

'Note for the guidance on validation of analytical procedures: Text and methodology' (1995) https://www.ema.europa.eu/en/documents/scientific-guideline/ich-q-2-r1-validation-analytical-procedures-text-methodology-step-5_en.pdf (Accessed: 06. March 2022).

Jade Institute – Chinese Herb Gallery

https://www.jadeinstitute.com/chinese-herbal-gallery/ (Accessed: 22. February 2022).

Jahoda, T. (2022). Analytical characterisation and isolation of a specialised white mulberry extract. Master's thesis. University of Vienna, Department of Pharmacognosy.

Langeder, J., Grienke, U., Chen, Y., Kirchmair, J., Schmidtke, M., & Rollinger, J. M. (2020). Natural products against acute respiratory infections: Strategies and lessons learned. *Journal of Ethnopharmacology*, *248*, 112298. https://doi.org/10.1016/j.jep.2019.112298

Li, X., Ren, Z., Wu, Z., Fu, Z., Xie, H., Deng, L., Jiang, X., & Chen, D. (2018). Steric Effect of Antioxidant Diels-Alder-Type Adducts: A Comparison of Sanggenon C with Sanggenon D. *Molecules*, *23*(10), 2610. https://doi.org/10.3390/molecules23102610

Morimura, A., Hamaguchi, S., Akeda, Y., & Tomono, K. (2021). Mechanisms Underlying Pneumococcal Transmission and Factors Influencing Host-Pneumococcus Interaction: A Review. *Frontiers in Cellular and Infection Microbiology*, *11*, 639450. https://doi.org/10.3389/fcimb.2021.639450

Rumpold, R. C. (2020). *Large-scale isolation and characterization of prenylated flavonoids from the root bark of Morus alba*. Diploma thesis. University of Vienna, Departement of Pharmacognosy. https://doi.org/10.25365/thesis.65096

Singh, R., Bagachi, A., & Semwal, A. (2013). *Traditional uses, phytochemistry and pharmacology of Morus alba Linn.: A review*. 9.

Song, G. R., Choi, Y. J., Park, S. J., Shin, S., Lee, G., Choi, H. J., Lee, D. Y., Song, G.-Y., & Oh, S. (2021). Root Bark of *Morus alba* L. and Its Bioactive Ingredient, Ursolic Acid, Suppress the Proliferation of Multiple Myeloma Cells by Inhibiting Wnt/β-Catenin Pathway. *Journal of Microbiology and Biotechnology*, *31*(11), 1559–1567. https://doi.org/10.4014/jmb.2109.09002

Walther, E., Xu, Z., Richter, M., Kirchmair, J., Grienke, U., Rollinger, J. M., Krumbholz, A., Saluz, H. P., Pfister, W., Sauerbrei, A., & Schmidtke, M. (2016). Dual Acting Neuraminidase Inhibitors Open New Opportunities to Disrupt the Lethal Synergism between Streptococcus pneumoniae and Influenza Virus. *Frontiers in Microbiology*, *7*. https://doi.org/10.3389/fmicb.2016.00357

Wang, Y.-N., Liu, M.-F., Hou, W.-Z., Xu, R.-M., Gao, J., Lu, A.-Q., Xie, M.-P., Li, L., Zhang, J.-J., Peng, Y., Ma, L.-L., Wang, X.-L., Shi, J.-G., & Wang, S.-J. (2017). Bioactive Benzofuran Derivatives from Cortex Mori Radicis, and Their Neuroprotective and Analgesic Activities Mediated by mGluR1. *Molecules*, *22*(2), 236. https://doi.org/10.3390/molecules22020236

Wei, H., Zhu, J.-J., Liu, X.-Q., Feng, W.-H., Wang, Z.-M., & Yan, L.-H. (2016). Review of bioactive compounds from root barks of *Morus* plants (Sang-Bai-Pi) and their pharmacological effects. *Cogent Chemistry*, *2*(1), 1212320. https://doi.org/10.1080/23312009.2016.1212320

Wen, P., Hu, T.-G., Linhardt, R. J., Liao, S.-T., Wu, H., & Zou, Y.-X. (2019). Mulberry: A review of bioactive compounds and advanced processing technology. *Trends in Food Science & Technology*, *83*, 138–158. https://doi.org/10.1016/j.tifs.2018.11.017

World Health Organization (WHO) (2018) Influenza Fact Sheets. Available at: http://www.who.int/mediacentre/factsheets/fs211/en/.
(Accessed: 25. February 2022).

World Health Organization (WHO) (2018) Vaccine-Preventable Diseases Surveillance Standards: Pneumococcus. Available at: https://www.who.int/immunization/monitoring_surveillance/burden/vpd/WHO_SurveillanceVaccinePreventable_17_Pneumococcus_R2.pdf?ua=1.
(Accessed: 27. February 2022)

World Health Organization (WHO) (2017) WHO Publishes List of Bacteria for Which New Antibiotics are Urgently Needed. Available at: https://www.who.int/newsroom/detail/27-02-2017-who-publishes-list-of-bacteria-for-which-newantibiotics-are-urgently-needed
(Accessed: 27. February 2022).

Yang, Y., Tan, Y.-X., Chen, R.-Y., & Kang, J. (2014). The latest review on the polyphenols and their bioactivities of Chinese *Morus* plants. *Journal of Asian Natural Products Research*, *16*(6), 690–702. https://doi.org/10.1080/10286020.2014.923405

Zafar, M. S., Muhammad, F., Javed, I., Akhtar, M., Khaliq, T., Aslam, B., Waheed, A., Yasmin, R., & Zafar, H. (2013). White mulberry (Morus alba): A brief phytochemical and pharmacological evaluations account. *Int. J. Agric. Biol.*, *15*, 612–620.

Zeng, Q., Chen, H., Zhang, C., Han, M., Li, T., Qi, X., Xiang, Z., & He, N. (2015). Definition of Eight Mulberry Species in the Genus Morus by Internal Transcribed Spacer-Based Phylogeny. *PLOS ONE*, *10*(8), e0135411. https://doi.org/10.1371/journal.pone.0135411

Zhu, Y.-P. (1998). *Chinese Materia Medica: Chemistry, pharmacology and applications*. CRC press.

REFERENCES OF FIGURES

Figure 1: Silkworm cocoon on mulberry leaf
https://www.abc.net.au/news/image/10633660-3x2-940x627.jpg
(accessed: February 2022)

Figure 2: Morus alba L.
https://www.mein-schoener-garten.de/sites/default/files/styles/achor_navigation_m/public/weiße-maulbeere-4317575-dam-fotolia.jpg?h=c029297a&itok=0opilUB-
(accessed: February 2022)

Figure 3: Sang Bai Pi
https://ae01.alicdn.com/kf/Hf14552dd1f3f4f1f93ecc0bd885466dcZ.jpg
(accessed: February 2022)

LIST OF ABBREVIATIONS

ACN	acetonitrile
ASE	accelerated solvent extraction
AUC	area under the curve
ddH_2O	double distilled water
ELSD	evaporative light scattering detector
HA	hemagglutinin
HPLC	high-performance liquid chromatography
ICH	International Council for Harmonisation of Technical Requirements for Pharmaceuticals for Human Use
IPA	isopropanol
LC-MS/MS	liquid chromatography tandem mass spectrometry
MAC130LS	a specialised *Morus alba* root bark extract generated by an accelerated solvent extraction on large scale
MAC1**	accelerated solvent extraction extracts
MAC0**	supercritical fluid extraction extracts
MeOH	methanol
NA	neuraminidase
PDA	photo diode array
SFE	supercritical fluid extraction
TCM	traditional Chinese medicine
UPLC	ultra-performance liquid chromatography
UHPLC	ultra-high-performance liquid chromatography
DAD-ESI-MS/MS	diode array detector electrospray ionization tandem mass spectrometry
WHO	World Health Organization

APPENDIX

*Figure A 1: Fragmentation pattern of lung sample 526 from sanggenon D [**2**]*

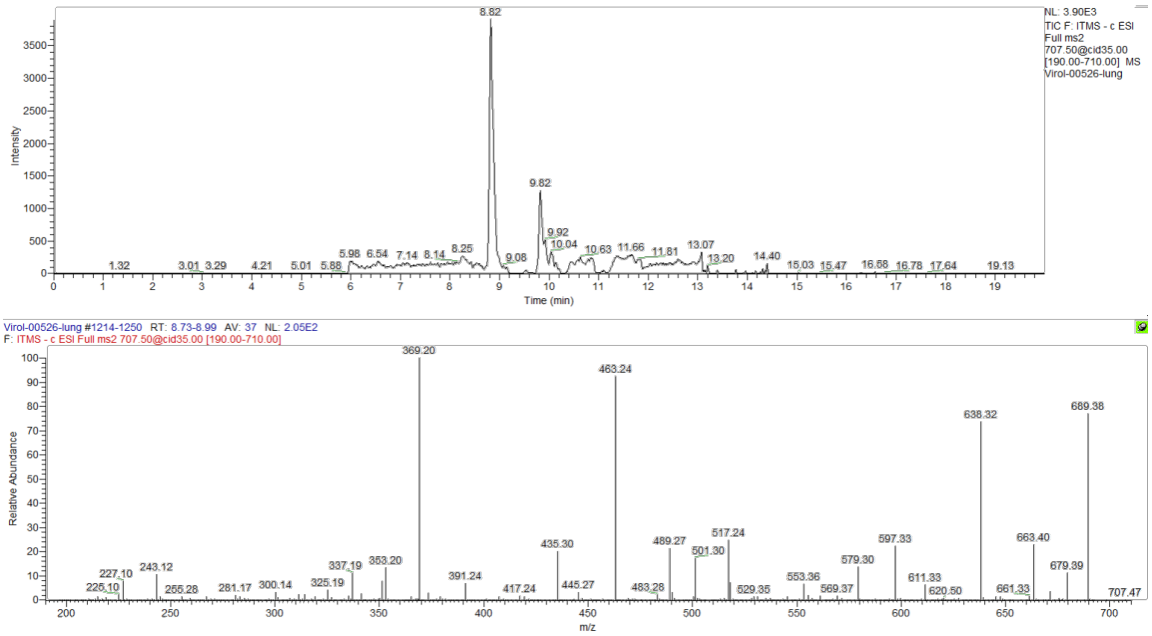

*Figure A 2: Fragmentation pattern of lung sample 529 from sanggenon D [**2**]*

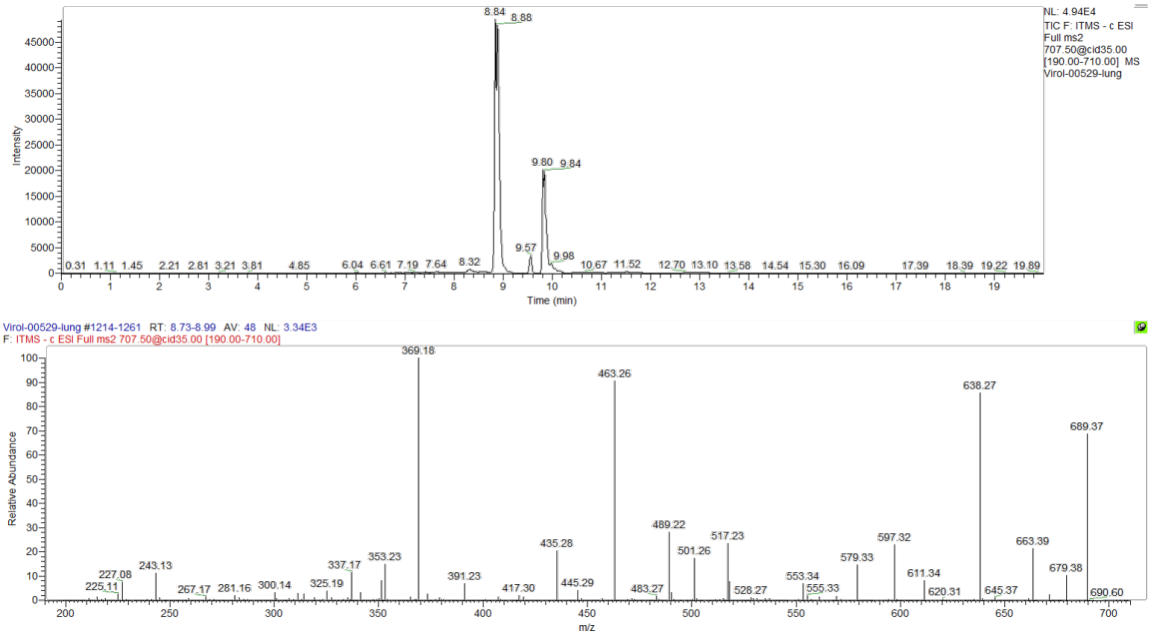

*Figure A 3: Fragmentation pattern of lung sample 529 from sanggenon C [**7**]*

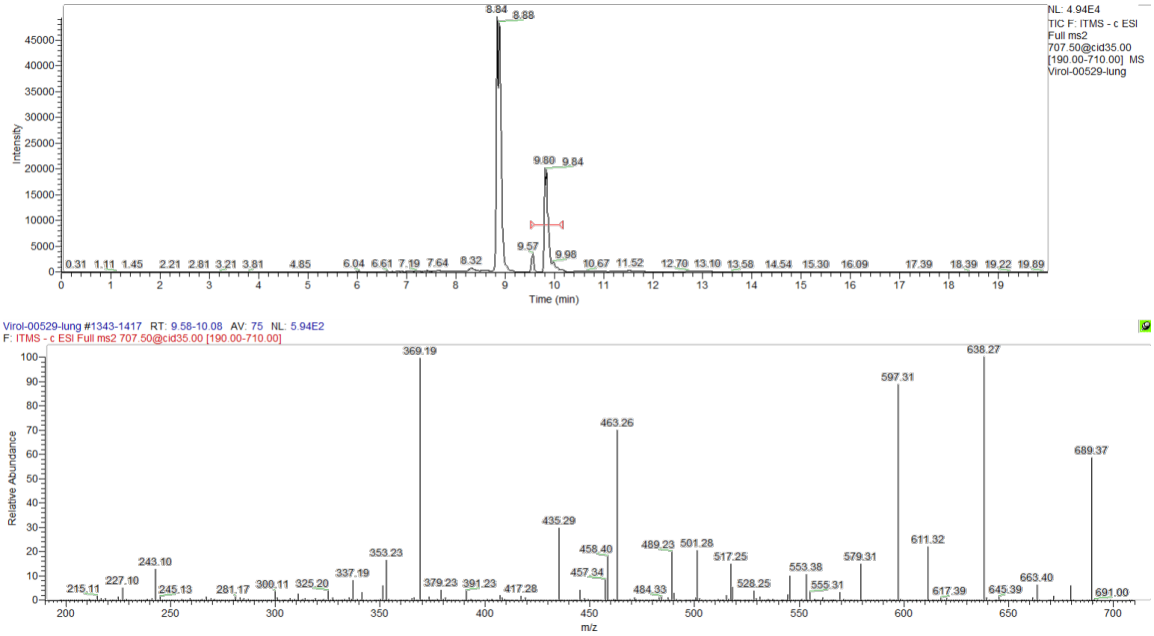

*Figure A 4: Fragmentation pattern of lung sample 532 from sanggenon D [**2**]*

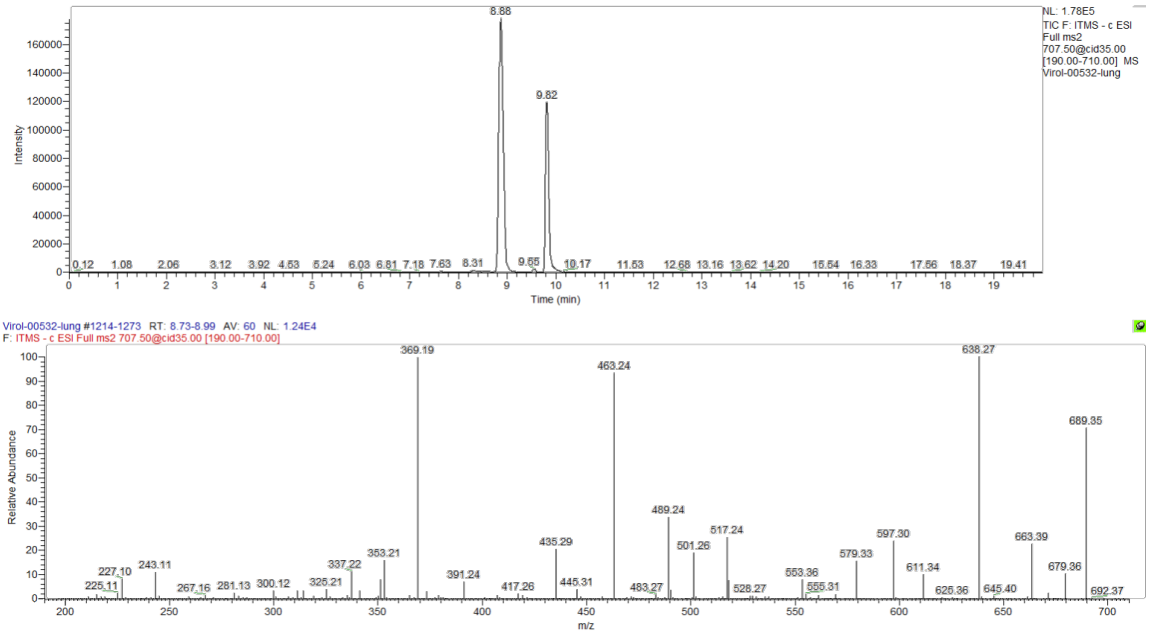

*Figure A 5: Fragmentation pattern of lung sample 532 from sanggenon C [**7**]*

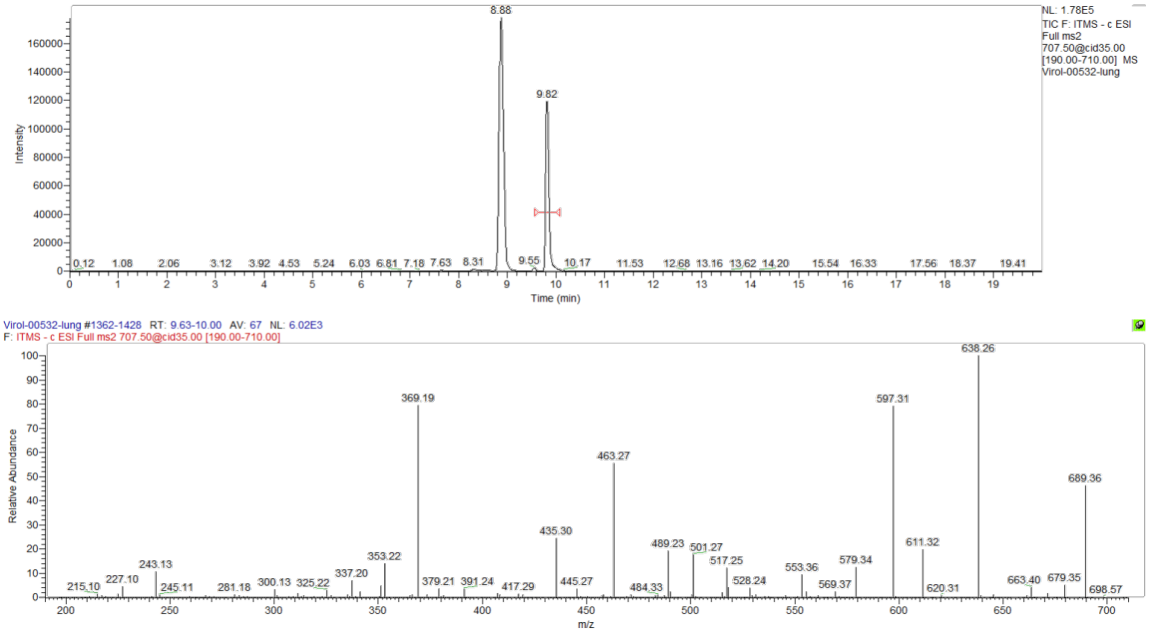

*Figure A 6: Fragmentation pattern of lung sample 533 from sanggenon D [**2**]*

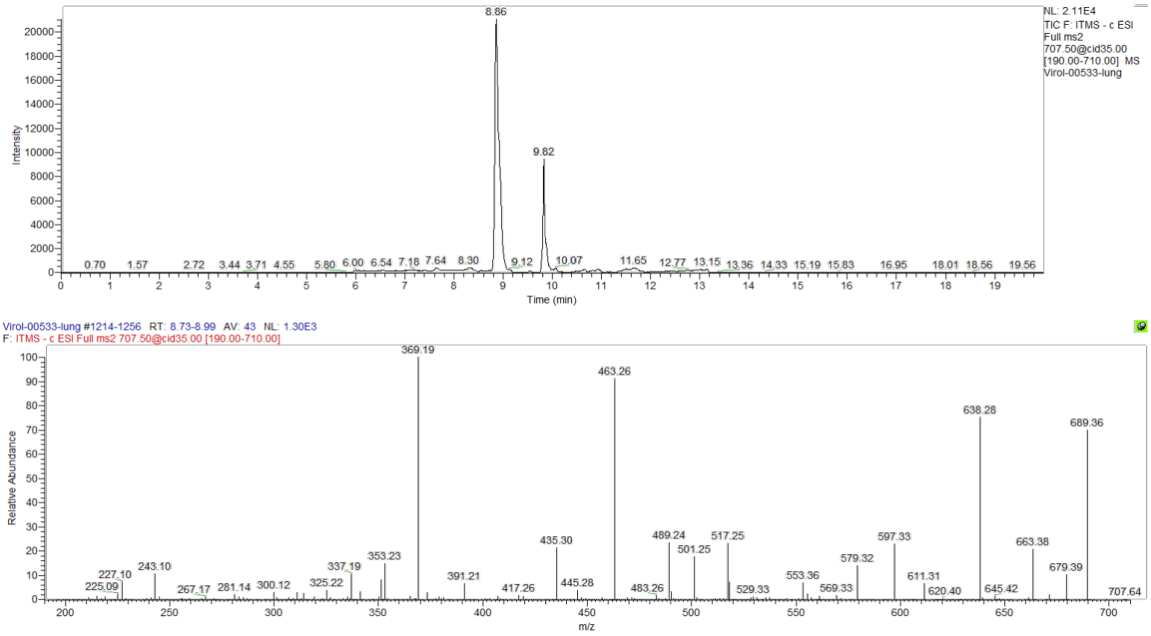

*Figure A 7: Fragmentation pattern of lung sample 535 from sanggenon D [**2**]*

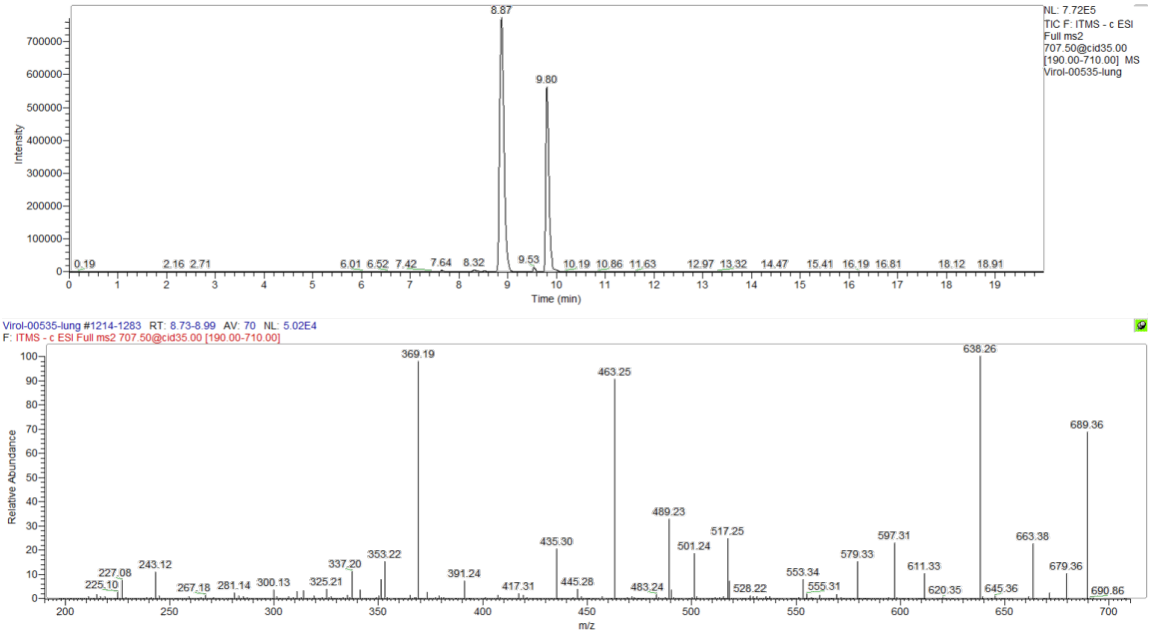

*Figure A 8: Fragmentation pattern of lung sample 535 from sanggenon C [**7**]*

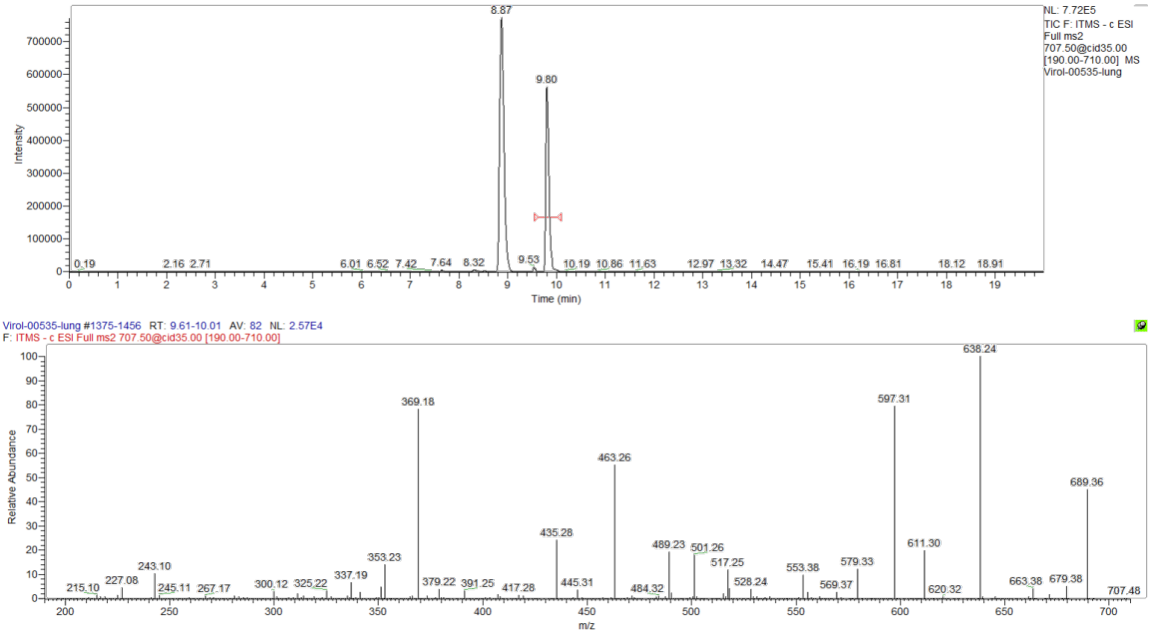

*Figure A 9: Fragmentation pattern of liver sample 532 from sanggenon D [**2**]*

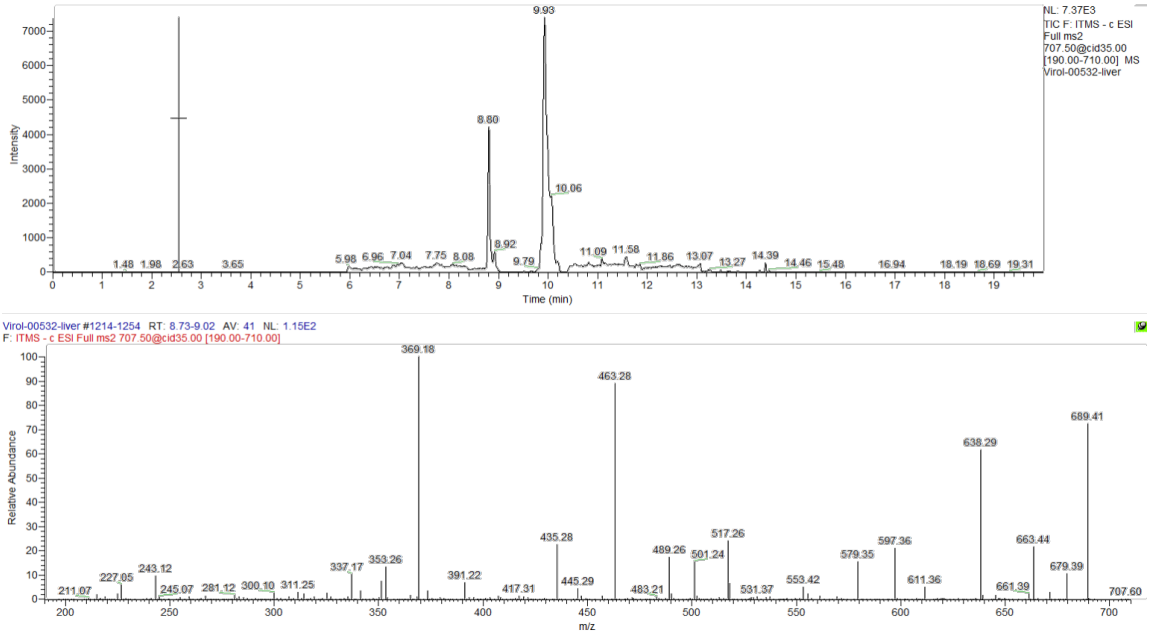

*Figure A 10: Fragmentation pattern of liver sample 538 from sanggenon D [**2**]*

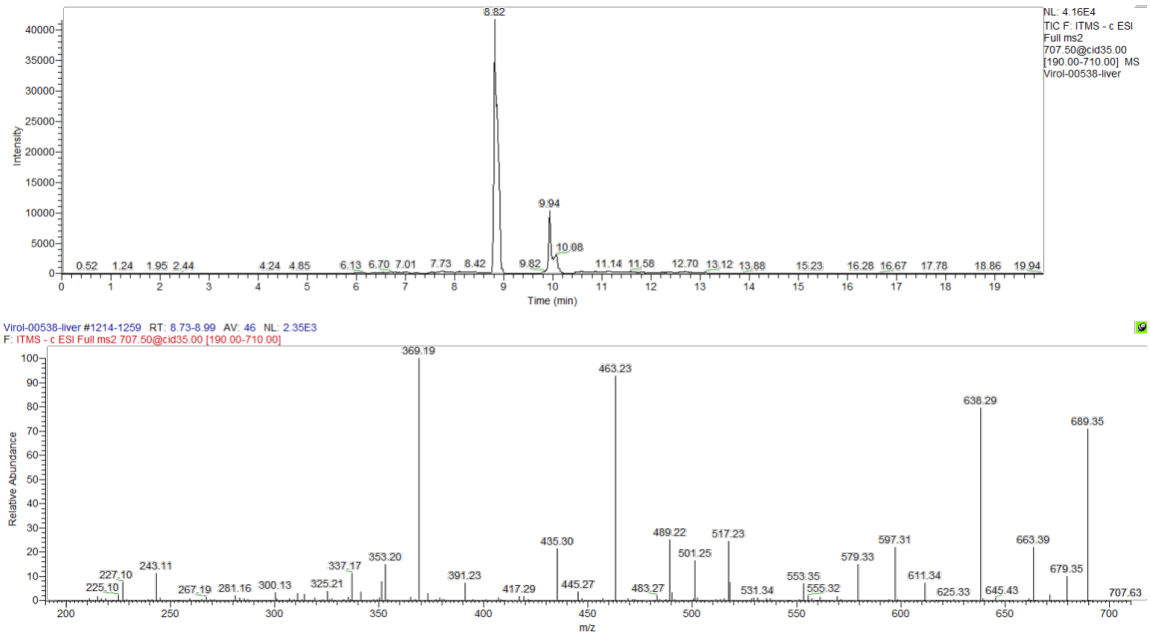

*Figure A 11: Fragmentation pattern of liver sample 539 from sanggenon D [**2**]*

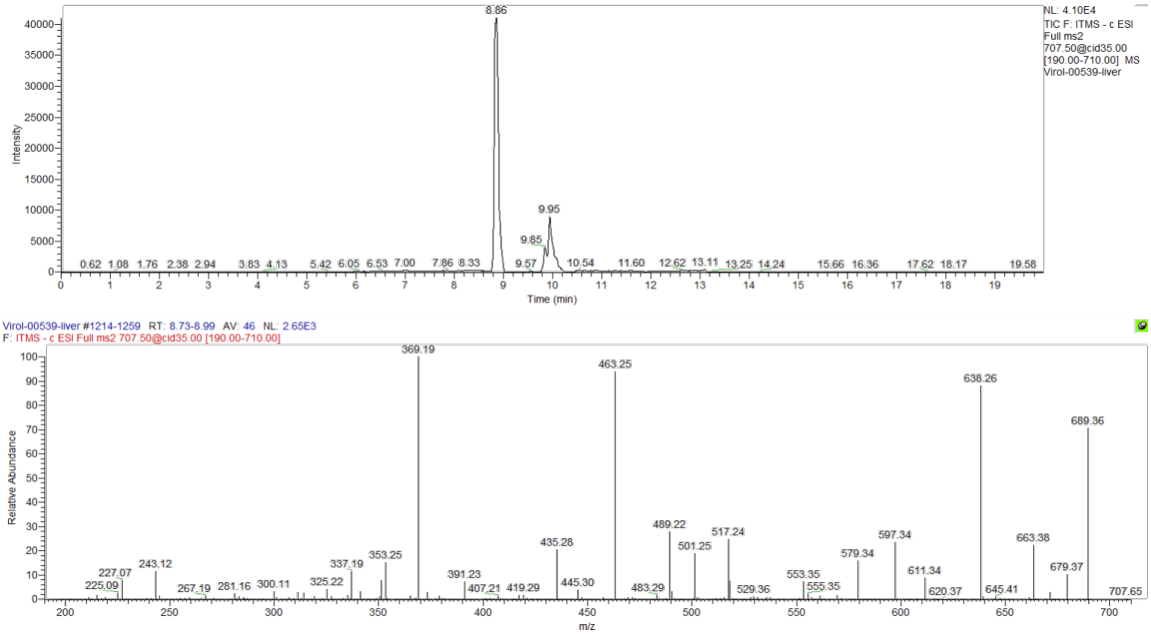

*Figure A 12: Fragmentation pattern of liver sample 534 from sanggenon D [**2**]*

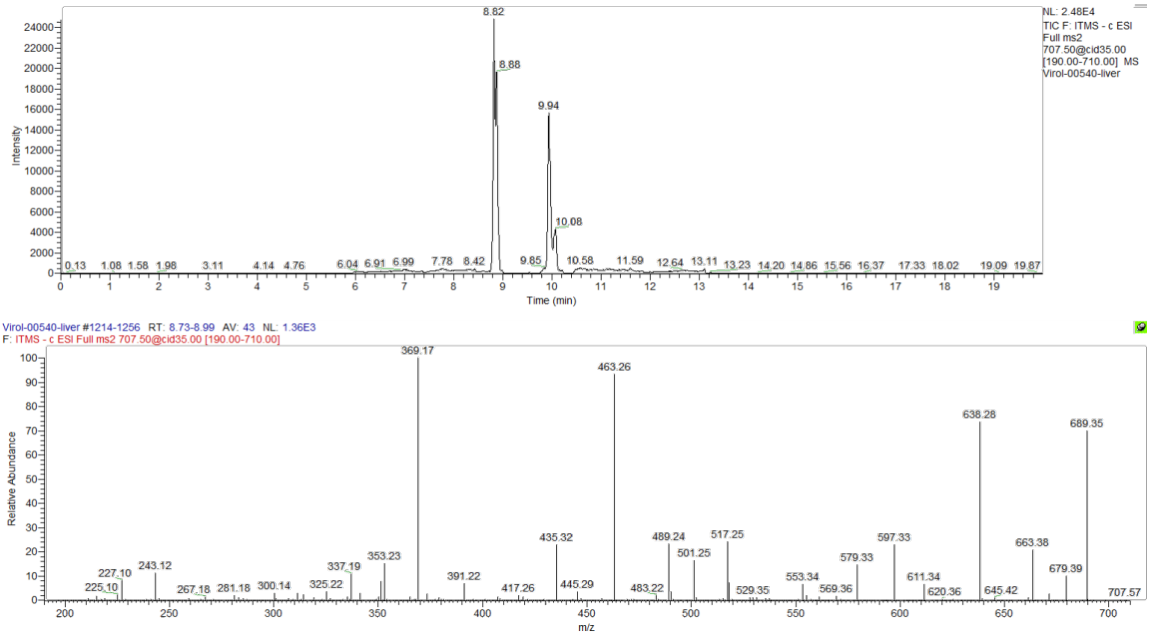

*Figure A 13: Fragmentation pattern of liver sample 564 from sanggenon D [**2**]*

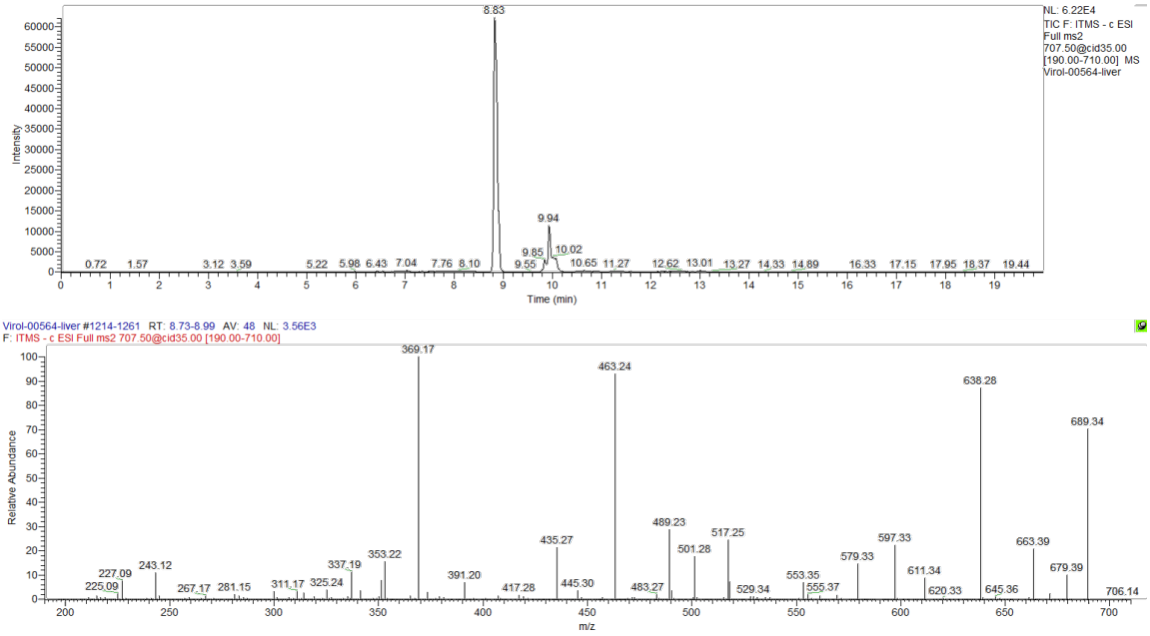

*Figure A 14: Fragmentation pattern of liver sample 565 from sanggenon D [**2**]*

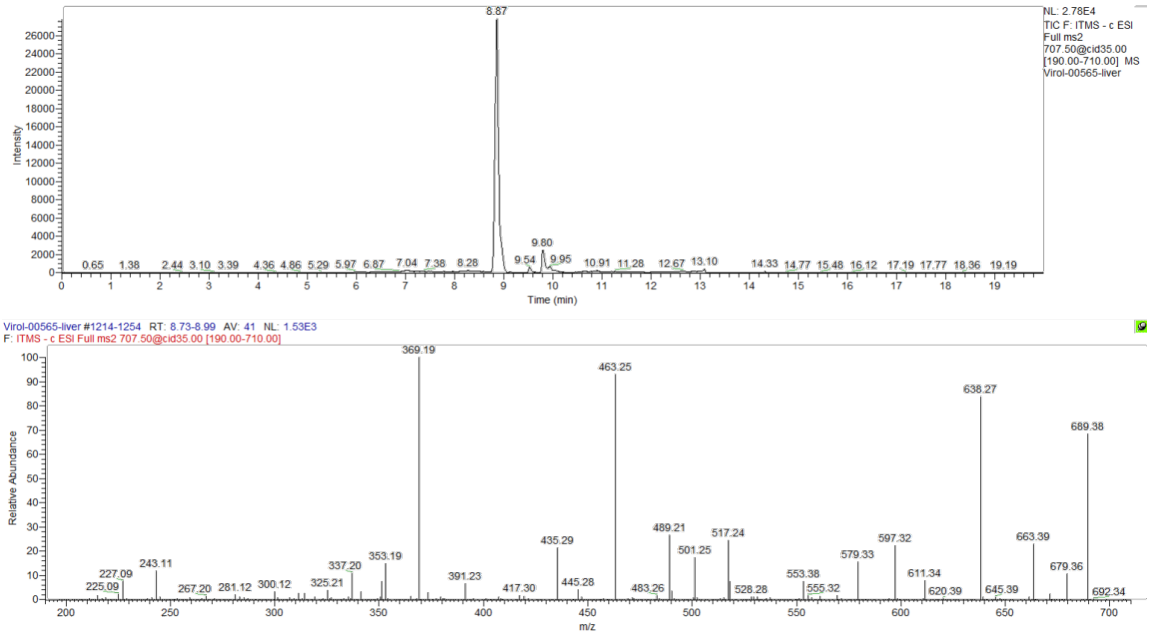

*Figure A 15: Fragmentation pattern of liver sample 566 from sanggenon D [**2**]*

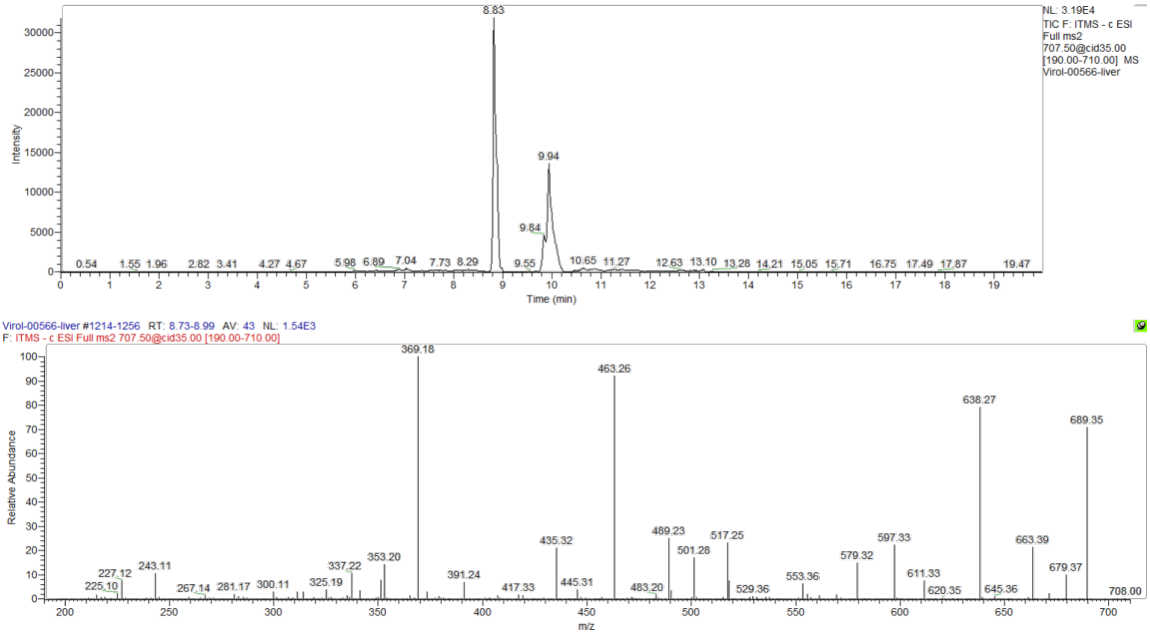

*Figure A 16: Fragmentation pattern of liver sample 566 from sanggenon C [**7**]*

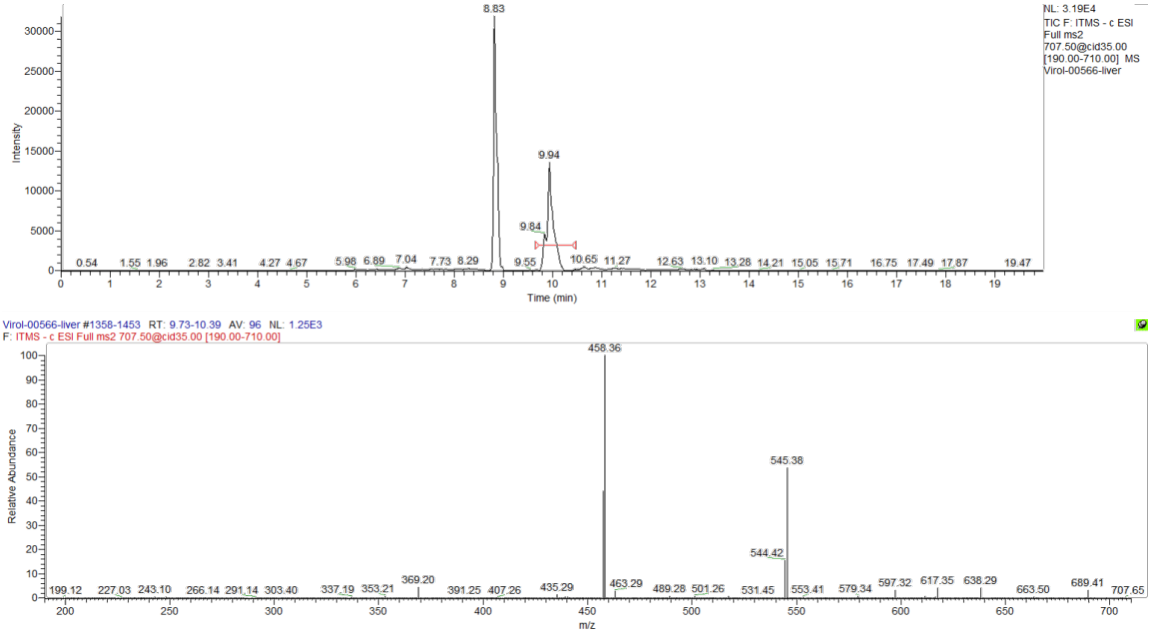

*Figure A 17: Fragmentation pattern of liver sample 567 from sanggenon D [**2**]*